Bioactive Materials 8 (2022) 177–195

Contents lists available at ScienceDirect

Bioactive Materials

journal homepage: www.sciencedirect.com/journal/bioactive-materials

Magnetostrictive alloys: Promising materials for biomedical applications

Chengde Gao [a], Zihao Zeng [a], Shuping Peng [b,c,**], Cijun Shuai [a,d,e,*]

[a] State Key Laboratory of High Performance Complex Manufacturing, College of Mechanical and Electrical Engineering, Central South University, Changsha, 410083, China
[b] NHC Key Laboratory of Carcinogenesis, The Key Laboratory of Carcinogenesis and Cancer Invasion of the Chinese Ministry of Education, School of Basic Medical Science, Central South University, Changsha, 410078, Hunan, China
[c] School of Energy and Machinery Engineering, Jiangxi University of Science and Technology, Nanchang, 330013, China
[d] Institute of Bioadditive Manufacturing, Jiangxi University of Science and Technology, Nanchang, 330013, China
[e] Shenzhen Institute of Information Technology, Shenzhen, 518172, China

ARTICLE INFO

Keywords:
Magnetostriction alloys
Magnetostriction theories
Preparation techniques
Measurement methods
Biomedical applications

ABSTRACT

Magnetostrictive alloys have attracted increasing attention in biomedical applications because of the ability to generate reversible deformation in the presence of external magnetic fields. This review focuses on the advances in magnetostrictive alloys and their biomedical applications. The theories of magnetostriction are systematically summarized. The different types of magnetostrictive alloys and their preparation methods are also reviewed in detail. The magnetostrictive strains and phase compositions of typical magnetostrictive alloys, including iron based, rare-earth based and ferrite materials, are presented. Besides, a variety of approaches to preparing rods, blocks and films of magnetostriction materials, as well as the corresponding methods and setups for magnetostriction measurement, are summarized and discussed. Moreover, the interactions between magnetostrictive alloys and cells are analyzed and emphasis is placed on the transduction and transformation process of mechanochemical signals induced by magnetostriction. The latest applications of magnetostrictive alloys in remote microactuators, magnetic field sensors, wireless implantable devices and biodegradable implants are also reviewed. Furthermore, future research directions of magnetostrictive alloys are prospected with focus on their potential applications in remote cell actuation and bone repair.

1. Introduction

Health has long been an unremitting pursuit of human beings. With the continuous improvement of living standards, great changes have taken place in people's understanding of health [1]. People are paying more and more attention to the therapy of diseases with higher requirements for the therapeutic methods and effects [2–6]. In view of this, increasing efforts have been devoted to developing novel medical technology and means. For example, surgical therapy has developed from open surgery to minimally invasive or even non-invasive surgery [7–11], and the repair of bone defects has developed from autogenous bone grafting and allogeneic bone grafting to artificial bone grafting, and even the in-depth research on biodegradable artificial bone, etc. [12–17]. These developments aim to achieve better therapeutic effect and reduce the accompanying adverse effects on patients' health. On this basis, the corresponding new therapeutic tools have also been rapidly developed, such as the applications of micro-electromechanical systems (MEMS) in cell operation, interventional therapy [18,19], and the development of new devices driven in vitro by electricity, machinery, and magnetism using the characteristics of smart materials [20–23].

As one kind of smart materials, magnetostrictive materials are capable of changing dimension under the action of external magnetic field and regaining the original dimension after removing the external magnetic field [24]. The attractive properties have drawn a wide range of research interests in biomedical fields. Early in 1992, a sensitive and reliable magnetostrictive sensor was developed for the monitoring of

Peer review under responsibility of KeAi Communications Co., Ltd.

* Corresponding author. State Key Laboratory of High Performance Complex Manufacturing, College of Mechanical and Electrical Engineering, Central South University, Changsha, 410083, China.

** Corresponding author. NHC Key Laboratory of Carcinogenesis, The Key Laboratory of Carcinogenesis and Cancer Invasion of the Chinese Ministry of Education, School of Basic Medical Science, Central South University, Changsha, 410078, Hunan, China.

E-mail addresses: shuping@csu.edu.cn (S. Peng), shuai@csu.edu.cn (C. Shuai).

https://doi.org/10.1016/j.bioactmat.2021.06.025
Received 18 April 2021; Received in revised form 1 June 2021; Accepted 22 June 2021
Available online 30 June 2021

articular movements and lung ventilation [25]. After that, Vargas-Esteve et al. studied the biocompatibility of Galfenol-based microparticles and proved their great potential as remote microactuators in cell biology and intracellular applications [26]. Moreover, Hart et al. innovatively investigated the use of magnetostriction in bone repair, in which magnetostriction materials were rigidly attached to a porcine tibia and then placed in an alternating magnetic field. Encouragingly, the results showed that magnetostriction could provide effective strain stimulation to increase and accelerate bone formation [27]. These studies demonstrated the great research and application potentials of magnetostriction in biomedical fields.

This review presents the research advances of magnetostrictive alloys and their cellular responses. The theories and mechanisms of magnetostriction are summarized and discussed in detail. Special attention is paid on the main categories, magnetostrictive performance and preparation methods of magnetostrictive alloys. The measuring methods for magnetostrictive properties are also introduced. Moreover, the biological performance of magnetostrictive alloys is also explored with a focus on the latest applications in remote cell drive. Finally, the future research directions of magnetostrictive alloys are prospected especially in remote cell actuation and bone repair.

2. Magnetostriction theories

2.1. Magnetostrictive effect

Magnetostriction is a phenomenon in which material is reversibly deformed when an external magnetic field is applied. Magnetostriction was first discovered in 1842 by Joule [28], so it was also called "Joule effect" as shown in Fig. 1 a. Then, in 1864, Villari discovered the reverse effect of magnetostriction, which was called "Villari effect" as shown in Fig. 1 b, i.e., the change of magnetization can be induced by the change in the length/volume of a magnetic material [29]. For engineering materials, magnetostriction is mainly concerned with the change in length (linear magnetostriction), which is the phenomenon of elongating or shortening along a certain direction driven by external magnetic field. The magnetostrictive capability is generally characterized by magnetostrictive strain λ ($\lambda = \Delta l/l$), in which Δl and l refer to the change in length and the original length of the material, respectively [30]. λ is a dimensionless quantity and generally expressed as $\times 10^{-6}$ or ppm [31]. If the magnetic material elongates, λ_s is positive, otherwise λ_s is negative. In addition, λ increases with the increase of magnetic field until a saturated value (λ_s), which is used to represent the saturated magnetostrictive properties of magnetic materials [32]. At room temperature, the λ_s of conventional magnetostrictive materials generally ranges from a few to tens of ppm, while the subsequently developed giant magnetostrictive materials exhibit λ_s of two orders of magnitude larger than conventional magnetostrictive materials [33].

2.2. Phenomenological theory

The magnetostriction of material is caused by the exchange coupling effect between the magnetic moments of adjacent atoms. When the distance between magnetic moments changes, the macroscopic behavior of the material appears as elongating or shortening [37]. In phenomenological theory, the coordinate axes are represented by x, y and z, and are consistent with the cubic crystal axes [100], [010] and [001], respectively. According to the symmetry of crystal and the principle of free energy, the magnetostriction of single crystal in the cubic crystal system can be expressed as [38]:

$$\lambda = \lambda^{\alpha} + \left(\frac{3}{2}\right)\lambda_{100}\left(\alpha_x^2\beta_x^2 + \alpha_y^2\beta_y^2 + \alpha_z^2\beta_z^2 - \frac{1}{3}\right) + 3\lambda_{111}\left(\alpha_x\alpha_y\beta_x\beta_y + \alpha_y\alpha_z\beta_y\beta_z + \alpha_z\alpha_x\beta_z\beta_x\right) \quad (1\text{-}1)$$

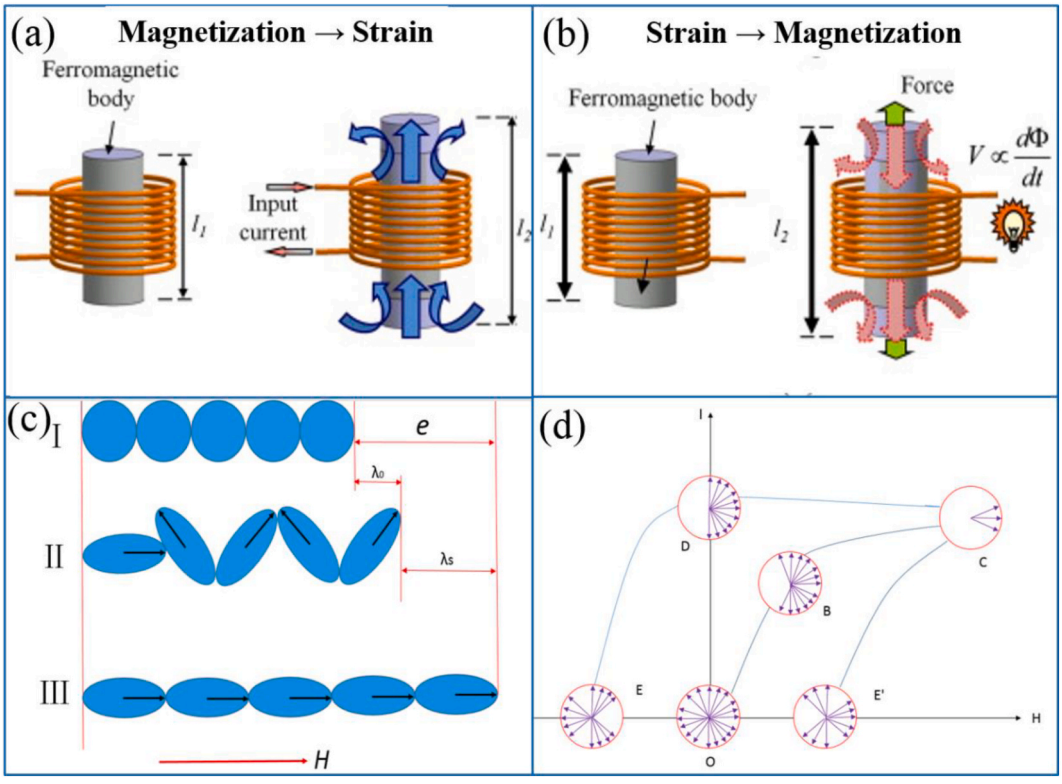

Fig. 1. Schematic descriptions of (a) Joule effect and (b) Villari effect. Reproduced with permission from Ref. [34] Copyright 2015 Elsevier (c) The magnetostriction of ferromagnetic materials: I. paramagnetic state above Tc; II. spontaneous magnetization after cooling below Tc; and III. saturated state in the presence of an external magnetic field. Reproduced with permission from Ref. [35] Copyright 2004 Researchgate. (d) The distribution of magnetic moments corresponding to different magnetization stages of ferromagnetic materials [36].

where the direction cosines of magnetization are α_x, α_y, α_z; the direction cosines of measurement are β_x, β_y, β_z; the magnetostriction along <100> and <111> directions are λ_{100} and λ_{111} respectively; λ^α is the deformation that does not vary with the direction of magnetization.

For isotropic ferromagnetic materials, $\lambda_{100} = \lambda_{111} = \lambda$, when λ^α is neglected, Formula 1-1 can be simplified as follows [38]:

$$\lambda = \left(\frac{3}{2}\right)\lambda_s\left(\cos^2\theta - \frac{1}{3}\right) \tag{1–2}$$

In the formula, θ represents the angle between the direction of magnetostriction measurement and the direction of magnetization, $\cos\theta = \alpha_x\beta_x + \alpha_y\beta_y\alpha + \alpha_z\beta_z$. When $\theta = 0°$, $\lambda = \lambda_s$ is the saturated magnetostrictive strain along the direction of magnetic field. Formula 1-2 is suitable for isotropic ferromagnetic materials and can be used to approximately calculate the magnetostriction of anisotropic ferromagnetic materials and polycrystalline materials with disordered grain orientation.

When ignoring the deformation λ^α, it can be proved that the λ_s of polycrystalline materials and its single crystal magnetostrictive strains (λ_{100} and λ_{111}) are in accord with the following formula [38]:

$$\lambda \approx \frac{2}{5}\lambda_{100} + \left(\frac{3}{5}\right)\lambda_{111} \tag{1–3}$$

2.3. Microscopic theory

2.3.1. The origin of magnetostriction for ferromagnetic materials

According to the principle of minimum free energy, the change of magnetization state in a material would induce the change of length/volume, which is a sufficient condition for the minimum total energy of the system. There are several mechanisms for the magnetostrictive phenomenon of magnetic materials:

(1) Spontaneous magnetostriction

Spontaneous magnetostriction is mainly caused by exchange forces (Fig. 1 c) [35]: I. Single-domain crystal appears spherical above its Curie temperature (Tc), when the temperature drops below Tc, the exchange force causes spontaneous magnetization of the crystal. II. Spontaneous magnetization makes the total atomic magnetic moment spin in the rotation direction and turn to a specific orientation, which would cause the pull-apart of nuclei and result in the spontaneous magnetization of λ_0. III. If the applied magnetic field is perpendicular to the direction of spontaneous magnetization, the direction of the total atomic magnetic moment would be parallel to external magnetic field, thus causing magnetostrictive strain of λ_s.

(2) Magnetostriction induced by magnetic field

The essence of magnetostriction is that the internal domains of ferromagnetic materials rotate and the magnetic domain walls move under the action of external magnetic field. Consequently, the energy of the system redistributes, making the total energy in the lowest state. The change of magnetoelastic properties leads to a change in the distance between adjacent atoms, which macroscopically appears as the elongating or shortening of material size. Magnetostrictive behavior is an external manifestation of the magnetization process of ferromagnetic materials. Therefore, the magnetostrictive performance depends on the magnetization process of the materials [39]. As shown in Fig. 1 d, the distribution of magnetic moments corresponds to different magnetization stages of ferromagnetic materials.

(3) Shape effect

For a spherical single domain sample, it is assumed that there only exists demagnetization energy ($1/2NM_S^2V$) without any spin-orbit coupling interaction or exchange [38]. In order to reduce the demagnetization energy, the sample volume should be shrunk accompanied by the decrease of demagnetization factor N via the elongation along magnetization direction. The shape effect caused by demagnetization energy is related to the shape of the magnetic material, and the resulting magnetostrictive effect is smaller than the aforementioned magnetostrictive effects [40].

(4) The origin of giant magnetostriction caused by rare earth ions

In rare earth-metals, -alloys and -intermetallic compounds, the giant magnetostrictive effect is mainly caused by the unfilled 4f layer electrons [41]. The 4f electron orbital of rare earth ions has strong anisotropy. When spontaneously magnetized, the 4f layer electrons will achieve the lowest energy in one or more specific directions. This causes large lattice distortion along these directions, resulting in giant magnetostriction [42].

2.3.2. Itinerant electron model based on band theory

Phenomenology theory can explain the macroscopic deformation of ferromagnetic materials caused by magnetostriction, but is incapable for the microscopic physical mechanisms. According to quantum theory, magnetostriction strain can be calculated according to the electronic structure, magnetic ions and crystal structure.

In itinerant electronic model, the magnetic 3d electrons are viewed as roaming, and the symmetry of crystals determines the space part of the wave function. The response energy can be expressed as $E_n(k)$, in which k denotes the state of electrons and n denotes the label of band. In non-ferromagnetic metals, each orbital of $E_n(k)$ has two electrons with opposite spin directions. In ferromagnetic metals, the 3d band is divided into two parts with different number of electrons due to the exchange interaction: one part spins up and the other part spins down, thus generating spontaneous magnetization. If the spin-orbit coupling is ignored, the direction of spontaneous magnetization is unrelated to the direction of crystal axis; otherwise, the direction of spontaneous magnetization is related to the direction of crystal axis, and thereby resulting in magnetostriction [43,44].

2.3.3. Single ion model based on local electrons

Single ion model can explain not only the magnetostriction of 3d, 4d and 5d metal ions in ferrites [45], but also the magnetostriction of 4f ions in rare earth alloys [46]. In this model, the vacant metal ions (magnetic ions) in the electronic shell of crystals are assumed as independent with each other. Moreover, the statistical average value of microscopic magnetocrystalline anisotropy energy for these metal ions is regarded as the macroscopic magnetocrystalline anisotropy energy for crystals. According to Boltzmann statistic theory, the relationship between macroscopic free energy density F and the microscopic energy of magnetic ions $E(\theta_i)$ follows the formula [38]: $F = -kT\sum_i N_i \ln Z_j$, $Z_j = \sum_i e^{-\frac{E_j(\theta_i)}{kT}}$, in which i represents different magnetic sublattices. N_i represents the number of magnetic ions on the i sublattice per unit volume. θ_i is the angle between the mean spin direction of magnetic ions on the i sublattice and the axis of symmetry of crystal field. $E_j(\theta_i)$ is the microscopic anisotropic energy of magnetic ions on the i sublattice, and $\sum_i$ is the sum of the quantum states of the magnetic ions on the i sublattice. This formula can be used to calculate the microscopic anisotropy energy of a single magnetic ion, and further the macroscopic anisotropy energy of crystals and then the magnetostriction of the alloys.

3. Magnetostrictive materials

Since the discovery of magnetostriction phenomenon in 1842, extensive work has been undertaken to develop magnetostrictive

materials and explore their applications (Table 1). Ferromagnetic materials, such as Fe, Ni, etc., are firstly developed magnetostrictive materials, which have saturated magnetostrictive strains in the range of 20–80 ppm [47–49]. Since the 1960s, rare earth magnetostrictive materials have been developed with saturated magnetostrictive strains of hundreds of times than those of Fe, Ni and other traditional magnetostrictive materials [50,51]. Afterwards, Terfenol-D ($Tb_{0.3}Dy_{0.7}Fe_2$) was developed in the 1970s and exhibited "giant" magnetostrictive strains in the range of 1000–2000 ppm [52]. In 2000, Fe–Ga alloy, another kind of giant magnetostrictive material without rare earth, has been extensively studied.

3.1. Magnetostrictive Fe–Ga alloys and Fe-Ga-X alloys

Fe–Ga alloys were developed by Clark et al. and became the most promising new magnetostrictive material due to their high magnetostrictive strain at low saturation field, low brittleness, high strength and excellent machinability [69–71]. Moreover, they were found to have great application potential in ultrasonic field, transducer, micro-displacement devices and magnetostrictive actuators. Yoo et al. studied the magnetostrictive patch transducer based on Fe–Ga alloy patch. In the case of a static magnetic field and a dynamic magnetic field created by applying alternating current (AC) to a coil, it was found that the direction sensing function of magnetostrictive patch transducer was significantly enhanced by Fe–Ga alloy patch [72]. Fe–Ga alloys have high tensile strength (~500 MPa), good thermal-mechanical properties and exhibit moderate saturated magnetostriction (~350 ppm) under low magnetic fields (~100 Oe), which fill the gap between traditional magnetostrictive materials and rare-earth giant magnetostrictive materials [73–75]. Thus, this section focuses on the magnetomechanical behavior of binary Fe–Ga alloys and ternary Fe–Ga alloys.

3.1.1. Fe–Ga alloys

The dissolution of Ga into bcc-Fe will form a substitutional solid solution [76]. When the atomic fraction of Ga in the substitutional solid solution increases continuously from 15% to 30%, a variety of phase structures like A2, $D0_3$, Ll_2, B2, $D0_{19}$ and Modified-$D0_3$ will emerge under different heat treatment conditions and directly affect the magnetostrictive properties of Fe–Ga alloys (Fig. 2 a) [54,77–80]. Among these phase structures, high-temperature disordered A2 phase contributes the most to the magnetostrictive property, and Modified-$D0_3$ phase can also improve the magnetoelastic coupling density of the alloys, but the appearance of ordered phase will greatly deteriorate the magnetostrictive property [55,81].

There is a general belief that the large magnetostriction of Fe–Ga alloys mainly comes from the Ga–Ga atom pairs and the unsymmetrical Ga clusters formed by replacing the neighboring Fe atoms in the direction of [100] in α-Fe bcc structure [82,83]. Clark et al. studied the relationship between Ga content and magnetostrictive properties of Fe–Ga alloys with single crystal [100] orientation. At low Ga contents, the alloys existed in the form of disordered A2 phase and ordered $D0_3$ phase. At this time, the saturated magnetostrictive strain increased with the increase of isolated Ga atom pairs. At high Ga contents, asymmetric Ga sub-clusters appeared and formed short-range order phases in the alloys, reducing magnetostriction [84,85]. Further study revealed that Fe–Ga alloys with Ga atomic fractions of 19% and 27.5% exhibited the best magnetostrictive properties. As shown in Fig. 2 b, magnetostrictive strain reached a peak value of about 400 ppm when the atomic fraction of Ga increased to 19%. This was because that the A2 phase, which was stable only at high temperature, could be retained at the room temperature after the quenching process. The second peak value occurred at the Ga atomic fraction of about 27.5%, which was mainly due to the very low shear modulus. Moreover, the alloy was almost entirely composed of $D0_3$ structure in this case [86].

3.1.2. Fe-Ga-X alloys

In recent years, scholars began to explore possible effective methods to further improve the magnetostrictive properties of Fe–Ga alloys. The addition of third elements to Fe–Ga alloys has been proven as a feasible method and one of the research hotspots in this field [71]. The effects of adding a third element can be broadly divided into the following categories:

- Enhancing the solid solubility limit of Ga atom in α-Fe-based solid solution and the stability of A2 phase;
- Improving the stability of $D0_3$ phase, reduces the solubility limit of Ga in α-Fe-based solid solution, and promotes the decomposition of A2 phase;
- Improving the plasticity and machinability of Fe–Ga alloys;
- Promoting the growth of some oriented grains in A2 phase and forming texture;
- Improving other physical properties of A2 phase, etc.

So far, the following four types of third elements have been added to Fe–Ga alloys through a lot of research.

(1) 3d and 4d transition elements (Ni, Mo, V, Cr, Mn, Rh, Co)

Many studies have investigated the effects of the addition of transition elements on the magnetostrictive properties of Fe–Ga alloys. The results showed that adding a small amount of Ni or Mo decreased both the values of λ_{111} and λ_{100} [57]. What's more, the addition of V, Cr, Mn or Rh was also disadvantageous to the magnetostrictive properties of Fe–Ga alloys (Fig. 2 c). The reason was that these elements had a stable effect on the $D0_3$ structure and would promote the formation of ordered $D0_3$ phase, which was not conducive to the magnetostrictive properties of Fe–Ga alloys [87]. However, the addition of Co showed some positive effects. The moderate substitution (<10%) of Co atoms for Fe atoms was found to increase the magnetostriction, magnetism and Tc of Fe–Ga alloys, which was a feasible way to improve the service temperature [88].

(2) Si, Ge, Sn and Al elements

In the periodic table, Si locates at the preceding period of Ga and has an empty d electronic shell, while Ge locates at the same period of Ga and has a full d electronic shell. Sn locates at the next period of Ga and has full 3d and 4d electronic shells. The three elements locate at three successive periods of the same group but show different effects on the magnetostrictive properties of Fe–Ga alloys. The substitution of a small amount of Sn slightly improves the magnetostrictive properties of the alloys [71]. However, the substitution of Si or Ge atoms for Ga atoms leads to the decrease of magnetostrictive properties of the alloys [89,90]. It is because that Si and Ge atoms can occupy the position of Ga atoms, forming large strains and hindering the formation of Ga–Ga atomic pairs. Al and Ga both belong to group IIIA with adjacent positions, showing similar atomic sizes and electronic configurations. Therefore, Ga atom and Al atom have similar effects on the expansion of lattice constant of Fe in Fe–Ga alloys. Researchers have found that the grain size of $Fe_{80}Ga_{20-x}Al_x$ ($x = 0, 6, 9, 14$) alloys increased while the magnetostrictive strain decreased with the increase of Al content. Moreover, the addition of Al can significantly promote the malleability of Fe–Ga alloys, for example, the elongation rate of the alloys increased from 1.3% to 16.5% after adding 9% Al [58].

(3) Interstitial elements (C, B, N)

The cubic lattice distortion in pure Fe caused by Ga atoms is believed to be helpful for improving the magnetostriction. For single crystal Fe–Ga alloys, it is found that small interstitial atoms, especially C, B and N, can get in the gap positions, which not only causes cubic lattice distortion but also inhibits the formation of stable $D0_3$ structures in the

Table 1
Typical magnetostrictive alloys.

Classification	Advantages	Mechanisms	Composition [Reference]	Preparation methods	Saturated magnetostriction	Saturation fields	Applications
Fe–Ga alloys	High magnetostrictive strain at low saturation field, low brittleness, high strength, excellent machinability	Suppression on the formation of metastable ($D0_3$) or stable ($L1_2$) ordered phases, and preservation of A_2 single-phase structure	$Fe_{81.6}Ga_{18.4}$ [26]	Magnetron sputtering method	~90 ppm	~10000 Oe	Remote cell actuation
			$Fe_{80}Ga_{20}$ [53]	Bridgman method	~300 ppm	_	Biodegradable mechanically active implants
			$Fe_{80.5}Ga_{19.5}$ [48]	Directional solidification method	~300 ppm	~200 Oe	Magnetostrictive actuators/sensors or energy harvesting applications
		The Ga–Ga atom pairs and the unsymmetrical Ga clusters formed by replacing the neighboring Fe atoms in Ref. [100] direction of α-Fe bcc structure	$Fe_{80}Ga_{20}$ [54]	Directional solidification method	~300 ppm	~3000 Oe	_
			$Fe_{80}Ga_{20}$ [55]	Rapid Quenching method	~700 ppm	~5000 Oe	Micro-displacement devices
			$Fe_{81}Ga_{19}$ [56]	Rolling method	~110 ppm	_	Ultrasonic fields
Fe-Ga-X alloys	Regulable magnetostrictive or other properties of Fe–Ga alloys	Stable effect on $D0_3$ structure and promoting the formation of ordered $D0_3$ phase	$Fe_{85}Ga_{10.2}Mo_{4.8}$ [57]	_	~117 ppm	~15000 Oe	_
		Altering the magnetic coupling of Fe atoms by non-magnetic elements with no d-shell electrons or full d-shell	$Fe_{80}Ga_{14}Al_6$ [58]	Directional solidification method	~205 ppm	~240 Oe	Transducer applications and magnetostrictive actuators
		Causing cubic lattice distortion and inhibiting the formation of stable $D0_3$ structure	$Fe_{78.92}Ga_{20.9}C_{0.18}$ [59]	Bridgman method	~432 ppm	_	Sensors
			AlN/FeGaB [60]	Magnetron sputtering method	~70 ppm	~152 Oe	Magnetic field sensors
		Stabilizing bcc-born (A2, B2 and $D0_3$) phases and preventing the appearance of closed packed (fcc ordered $L1_2$ and hcp ordered $D0_{19}$) phases, as well as increasing the number of grains in <100> orientation	$(Fe_{0.83}Ga0.17)_{99.75}Dy_{0.25}$ [61]	Melt-spun method	~620 ppm	~15000 Oe	Magnetoelectric (or multiferroic) sensors and transducers
Fe–Al alloys	High magnetomechanical coupling strain and low eddy current losses	_	$Fe_{80}Al_{20}$ [62]	Magnetron sputtering method	~55 ppm	~1000 Oe	Commercial energy harvesters
Fe–Co alloys	High magnetostrictive properties at room temperature, as well as good ductility, very soft magnetic properties and low saturation magnetic field	The precipitation of fcc Co-rich grains into the bcc α-Fe matrix	$Fe_{30}Co_{70}$ [63]	Rolling method	~116 ppm	~1200 Oe	Actuators and power generation devices
Fe–Pd alloys	Unique martensitic transformation and shape memory effects	The dispersion of strain glass with strain nanodomains into the austenite matrix	$Fe_{67.7}Pd_{32.3}$ [64]	Directional solidification method	~800 ppm	~800 Oe	Micromechanical and intelligent material systems controlled by magnetic fields
Tb–Fe alloys and Dy–Fe alloys	A huge cubic magnetic anisotropy at room temperature as well as large magnetostriction	Large strain-dependent anisotropy of the rare-earth ion situated at the cubic sites in the RFe_2 lattice.	$TbFe_2$ [65]	Directional solidification method	~1800 ppm	~10000 Oe	Magnetomechanical transducers, actuators and adaptive vibration control systems
Tb-Dy-Fe alloys	Low anisotropy and giant magnetostrictive strains at room temperature	Magnetic anisotropy of Dy and Tb: similar in magnitude but	$(Tb_{0.27}Dy_{0.73})_{1.04}Fe_{1.95}$ [66]	Directional solidification method	~2015 ppm ~900 ppm	~5000 Oe	Sonar systems, precision control systems, various valves

(*continued on next page*)

Table 1 (*continued*)

Classification	Advantages	Mechanisms	Composition [Reference]	Preparation methods	Saturated magnetostriction	Saturation fields	Applications
		opposite in direction at room temperature	Tb-Dy-Fe/epoxy composites [27]	Bongding method		~20000 Oe	Strain stimulation to increase and accelerate bone formation
			Tb-Dy-Fe/poly(vinylidene fluoride-co-trifluoroethylene) composites [67]	_	~110 ppm	~500 Oe	Remote mechanical stimulation to enhance cell proliferation
Ferrite materials	Strong magnetism, high electrical resistance and low eddy current losses	The presence of small and uniform grains without substantial grain growth	$CoFe_2O_4$ [68]	Combustion method	~197 ppm	~5000 Oe	Permanent magnets, drug delivery, microwave devices and high-density information storage

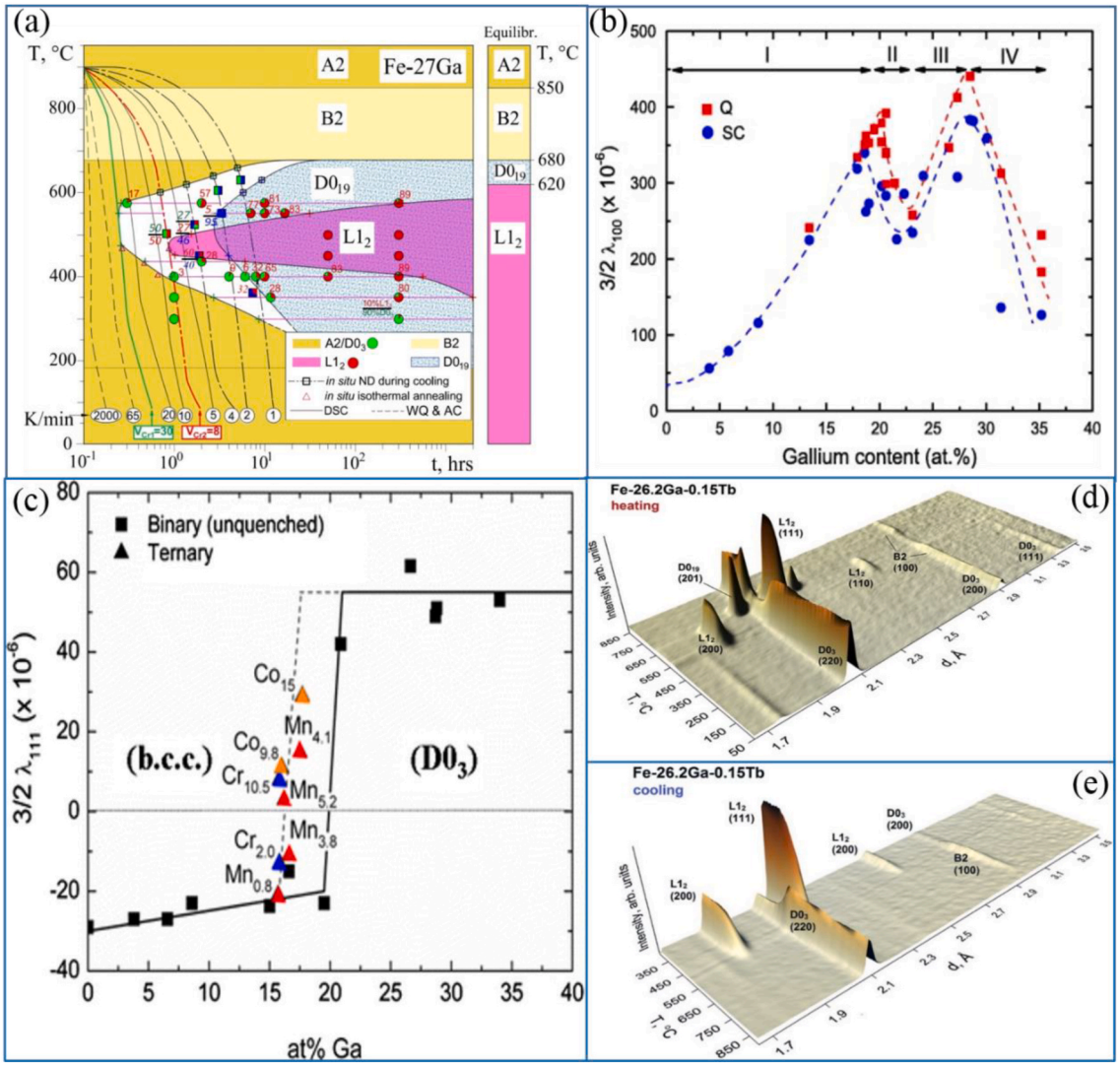

Fig. 2. (a) The Time-Temperature-Transformation diagram for Fe-27Ga alloy. The first and second critical cooling rates are represented by thick green and red lines, respectively. The X-ray diffraction (XRD) results are shown by a Pie chart with horizontal lines presenting the lever rule, and the lines for different cooling rates are shown in K/min. The plus-shaped points are derived from the in situ neutron diffraction isothermal annealing or from the XRD results. Reproduced with permission from Ref. [80] Copyright 2020 Elsevier. (b) Saturated magnetostriction of Fe–Ga alloys as a function of Ga content showing four regimes I ~ IV as arrowed. Q: water-quenched from 1000 °C; SC: slow-cooled at 10 °C min−1 from 1000 °C. Reproduced with permission from Ref. [86] Copyright 2008 Elsevier. (c) Saturated magnetostriction 3/2 λ_{111} for Fe–Ga binary system and Fe–Ga ternary systems with the addition of Cr, Mn, or Co. Reproduced with permission from Ref. [87] Copyright 2007 AIP. The three-dimensional (3D) visualization of the diffraction pattern upon (d) heating and (e) subsequent cooling of Fe-26.2Ga-0.15 Tb alloys after direct solidification. Reproduced with permission from Ref. [95] Copyright 2017 Elsevier. (For interpretation of the references to colour in this figure legend, the reader is referred to the Web version of this article.)

alloys, thereby improving the magnetostriction of single crystal Fe–Ga alloys. Dong et al. developed a highly sensitive sensor by taking advantages of the high saturation magnetostriction and low anisotropy of FeGaB alloy and the magnetically annealed FeGaB films can achieve a high saturation magnetostriction of 75 ppm at a low saturation field of 12 Oe [91]. However, for polycrystalline Fe–Ga alloys, the addition of C, B small interstitial atoms significantly reduce the magnetostrictive properties of the alloys [59,92].

(4) Rare earth elements

Rare earth elements can improve the magnetic properties of most materials because of their empty 4f electronic layer [93]. The earliest discovered giant magnetostrictive material was $Fe_{83}Ga_{17}$ alloy doped with a small amount of Tb [94]. The doping of Tb stabilized bcc-born (A2, B2 and $D0_3$) phases and prevented the appearance of closed packed (fcc ordered $L1_2$ and hcp ordered $D0_{19}$) phases (Fig. 2 d and e), as well as increased number of grains in <100> orientation and thereby improved magnetostrictive properties [95]. Moreover, studies have also shown that the addition of rare earth Dy would not change the original bcc-Fe structure of Fe–Ga alloys. Dy mainly enriched at the grain boundary and formed precipitated phase, while Ga in the matrix was biased towards the rare earth phase containing Dy. What's more, the addition of Dy significantly increased the <100> preferred orientation of Fe–Ga polycrystalline alloys, thus increasing the magnetostrictive strain [61,96]. Further research found that the best-doped elements were light rare earth elements such as Pr, La, etc., and the vertical magnetostriction could reach −800 ppm, which was five times of the magnetostrictive properties before doping [97,98]. These studies open up a new direction for the development of new giant magnetostrictive materials.

3.2. Other magnetostrictive Fe-based alloys

3.2.1. Fe–Al alloys

Since 1928, Fe–Al alloys have been developed as potential magnetostrictive materials. It was found that the characteristics of Fe–Al alloys were similar to those of Fe–Ga alloys in many aspects. On the one hand, the saturated magnetostriction λ_{100} of Fe–Al alloys occurred at the Al content of 19 at.%, which bore a striking resemblance to that of Fe–Ga alloys (Fig. 3 a) [62]. On the other hand, the phase diagram of binary Fe–Al alloys (Fig. 3 b) was also very similar to that of Fe–Ga alloys in the iron-rich region [99]. Therefore, it is expected to obtain Fe–Al magnetostrictive materials with excellent comprehensive properties. Pigott first discovered large magnetostriction in Fe–Al alloys containing 13 at. % Al in 1956 [100]. Afterwards, these alloys, known as Alfenol, are commonly used in commercial energy harvesters owing to high magnetomechanical coupling strain and low eddy current losses [101], Moreover, they also presented higher hardness and strength, smaller density and lower cost compared with other Fe-based alloys [102].

3.2.2. Fe–Co alloys

Fe–Co alloys exhibit high magnetostrictive properties at room temperature, as well as good ductility, very soft magnetic properties and low saturation magnetic field [103,104]. Compared with Fe–Ga alloys, Fe–Co alloys have abundant resources and lower cost, making them good candidates for various applications in actuators and power generation devices [105]. Fig. 3 c shows the relationship between the atomic percent of Co and saturated magnetostriction of Fe–Co alloys prepared by different methods. As can be seen, there are two peaks in the λ_s of the alloys with Co percent of 70% and 45%, respectively. The maximum magnetostrictive strain of $Fe_{30}Co_{70}$ alloy is about 92 ppm while that of $Fe_{55}Co_{45}$ alloy is 80 ppm. The alloy exhibits the lowest

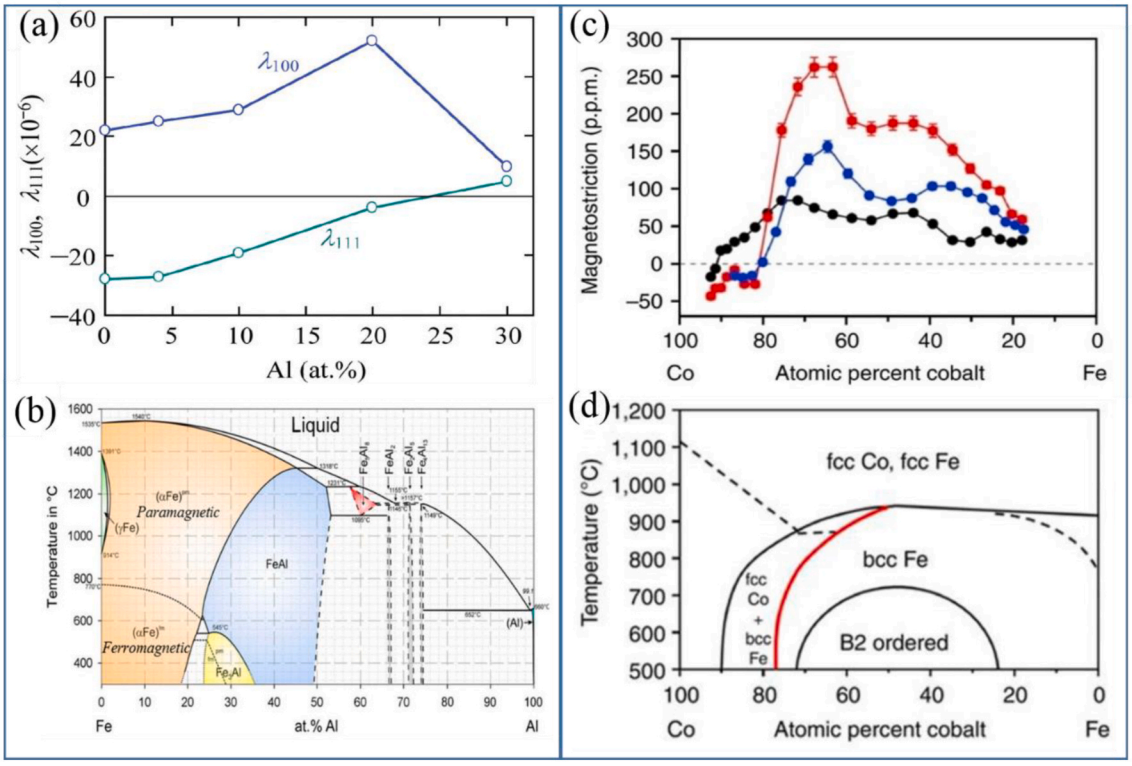

Fig. 3. (a) Magnetostriction constants, λ_{100} and λ_{111}, of Fe–Al (001) single-crystal films as a function of Al content. Reproduced with permission from Ref. [62] Copyright 2016 AIP (b) Fe–Al phase diagram. In the phase diagram, some of the solubility lines are plotted with dashed lines because they are still not well determined. Reproduced with permission from Ref. [99] Copyright 2016 MDPI. (c) Saturated magnetostriction versus the atomic percent of Co for Fe–Co alloys prepared by different methods: as-deposited (black dots), slow-cooled (blue dots) and quenched (red dots). (d) Fe–Co-phase diagram. The red curve highlights the approximate phase boundary between (fcc Co + bcc Fe) and bcc Fe. Reproduced with permission from Ref. [106] Copyright 2020 MDPI. (For interpretation of the references to colour in this figure legend, the reader is referred to the Web version of this article.)

magnetostrictive strain of 50 ppm when the atomic percent of Co is 55%. The magnetostriction of Fe–Co alloy is also related to the cooling process, and the maximum magnetostriction is found at the (fcc + bcc)/bcc phase boundary (Fig. 3 d). The results show that the magnetostrictive enhancement is caused by the precipitation of fcc Co-rich grains into the bcc α-Fe matrix, which is the same as the precipitation of $D0_3$ in Fe–Ga alloy [106]. It was also reported that the maximum strain in Fe–Co films could reach 130 ppm, which was attributed to the softening of elastic modulus in the alloys with high Co percent [63]. Moreover, Wang et al. developed a CoFeC alloy film with a high saturation magnetostrictive constant of 75 ppm, a high voltage electromagnetic coefficient of 10.3 ppm/Oe and a low coercivity lower than 2 Oe. The high saturation magnetostrictive constant and piezoelectric coefficient were caused by the coexistence of cubic phase and amorphous phase in the center of the nanocrystalline [107].

3.2.3. Fe–Pd alloys

Fe–Pd alloys have attracted extensive attentions in micromechanical and intelligent material systems controlled by magnetic fields due to their unique martensitic transformation and shape memory effects [108]. More recently, they have come into view again because of their excellent magnetostrictive properties under low magnetic fields. Ren et al. found a low-field-triggered large magnetostriction in Fe–Pd alloys, which showed a magnetostrictive strain of 800 ppm at a saturation field of 0.8 kOe when the concent of Pd was 32.3 at.% [64]. Moreover, Kubota et al. also found a large magnetostriction about 650 ppm in rapid-solidified Fe-29.6 at.% Pd alloy [109]. The large magnetostriction of Fe–Pd alloys is mainly due to two reasons: one is that magnetic field influences the reorientation of martensite twins and the other is the martensitic transformation in Fe–Pd alloys.

3.3. Magnetostrictive rare earth-based alloys

3.3.1. Tb–Fe alloys and Dy–Fe alloys

In the 1960s, it was discovered that most of the rare-earth metals exhibited great magnetostriction below Tc, but their Tc were much lower than room temperature and showed low magnetostriction at room temperature [110]. Therefore, many studies have been done to develop alloys possessing large magnetostriction with higher Tc. Clak et al. increased the Tc of heavy rare-earth metals Tb and Dy by alloying magnetic transition metals Fe, Co and Ni. Moreover, the resulting $TbFe_2$, $DyFe_2$ and other binary rare earth compounds exhibited cubic Laves structure [111,112]. The room temperature magnetostriction value of $TbFe_2$ single crystal was more than 2600 ppm along the easy magnetization direction <111> [113]. However, $TbFe_2$ and $DyFe_2$ alloys in cubic Laves structure had large anisotropy which indicated that they could produce large magnetostrictive strain only under the action of a large magnetic field (more than 800 kA/m), which limited their practical applications [65].

3.3.2. Tb-Dy-Fe alloys

The magnetostrictive Tb-Dy-Fe alloys are generally written as $Tb_{1-x}Dy_xFe_2$ where x defines the concentration of Dy. And when $x = 0.7$, the $Tb_{0.3}Dy_{0.7}Fe_2$ alloy, which is generally called Terfenol-D, owns the lowest room temperature anisotropy [114]. The saturation magnetization field of Terfenol-D is less than 80 kA/m, which is much smaller than those of $TbFe_2$ and $DyFe_2$ alloys [115]. The reason is that the magnetic anisotropy of Dy and Tb is similar in magnitude but opposite in direction at room temperature. Therefore, the addition of both Dy and Tb to Fe matrix leads to much low anisotropy and large magnetostrictive strains of Terfenol-D at room temperature. Moreover, recent studies have shown that Terfenol-D possessed positive magnetostrictive strains in excess of 2000 ppm after heat treating in a strong magnetic field. And the change in magnetostriction is linked to the alteration of the light and dark contrast in the domain image induced by high magnetic fields [66]. Nowadays, Terfenol-D is the most widely used magnetostrictive materials in various fields, such as sonar systems, high-power ultra-large ultrasonic devices, precision control systems, various valves and so on. However, the wider application of Terfenol-D is seriously limited by the presence of high eddy current loss when the frequency is above a few kHz. Wan et al. studied the magnetostrictive properties of Terfenol-D/epoxy and piezoelectric lead–zirconate–titanate [$Pb(Zr_{0.52}Ti_{0.48})O_3$]/epoxy composites under AC and found that the eddy current loss of this composite was negligible when the frequency as high as ~200 kHz due to the effective ME coupling between the two components [116]. In another study, the number of 180° domain walls in magnetostrictive material was increased by the oblique field annealing method, which reduced the eddy current loss of the magnetostrictive material at high frequency (especially effective in the frequency range around 50 Hz - 20 kHz) [117]. In addition, the high price, high magnetization field, brittleness and difficulty in machining should also be concerned for the applications of Terfenol-D [115].

3.4. Magnetostrictive ferrite materials

Ferrite materials are composite oxides consisting of iron oxides and one or more other metal oxides. Most of the ferrite materials have strong magnetism, high electrical resistance and low eddy current losses. And further studies showed that some ferrite materials exhibited well magnetostrictive strains together with high Tc [118,119]. Because of these excellent properties, ferrite nanoparticles have been widely used in permanent magnets, drug delivery, microwave devices and high-density information storage [120]. Many experiments have been done to study the different components of ferrite materials. It was found that most ferrite materials exhibited small magnetocrystalline anisotropy constant and magnetostrictive strain [121]. However, cobalt ferrite showed different characteristics with larger magnetostrictive strain and controllable magnetocrystalline anisotropy constant [45]. In 2007, the magnetostrictive strain of sintered cobalt ferrite was found to reach −197 ppm [68], and subsequent research reported a magnetostrictive strain of −400 ppm for polycrystalline cobalt ferrite [122]. Based on these characteristics, researchers have been full of expectations for cobalt ferrite magnetostrictive materials to replace rare earth magnetostrictive materials.

4. Preparation and measurement methods of magnetostrictive alloys

4.1. Preparation methods

The magnetostrictive properties of the materials are closely related to their microstructure [123,124]. Since the 1970s, magnetostrictive materials have been prepared by directional solidification, rolling, bonding, etc. and the microstructure of materials can be optimized by selecting appropriate preparation method to obtain magnetostrictive materials with better properties [125].

(1) Directional solidification methods

Directional solidification is the most commonly used method for preparing metallic magnetostrictive materials, such as Fe-based and rare earth-based magnetostrictive materials. This method can be used to prepare polycrystalline magnetostrictive materials with large size, regular surface, uniform axial composition and properties. Directional solidification methods are based on the principle of competitive grain growth to obtain large magnetostrictive materials with preferred orientation. The columnar or even single crystal can be obtained by directional solidification, which greatly improves the magnetostrictive properties of materials [126–128]. Directional solidification methods mainly include floating zone method, Czochralski method, and Bridgman method according to specific processes [114].

The floating zone method (Fig. 4 a) is the main preparation method

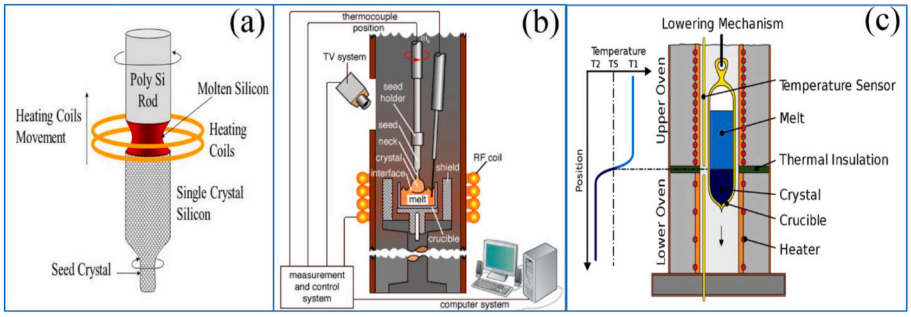

Fig. 4. Schematic setups for directional solidification methods. (a) Floating zone method, (b) Czochralski method, (c) Bridgman method.

(2) Rolling method

of small size magnetostrictive materials [129]. It can not only avoid the contamination of crucible to raw materials, but also reduce the burning loss of elements. However, this method has two main shortcomings. One is that it is difficult to get fault-free crystals due to the complex interface between the melt and crystal. The other is the high cost because this method requires high pure polysilicon rods as raw materials [130]. The main advantage of Czochralski method (Fig. 4 b) is that the crystal growth can be directly observed and the crystal diameter can be controlled. What's more, comparing with other crystal growth methods, the crystal grows faster with lower crystal dislocation density and higher optical homogeneity [131,132]. For Bridgman method (Fig. 4 c), if the moving speed of induction coil and the critical solidification speed are controlled properly, high performance magnetostrictive rod can be fabricated [101]. This method is highlighted by the capability of preparing large diameter materials [133]. However, it is easy to cause the loss of raw materials due to the slow downward pumping during the heating process [134].

Rolling method (Fig. 5 a) drags the alloy into the roll gap via the friction between the roll and the alloy, so that the alloy is compressed, resulting in a reduced section and an increased length [135]. The rolling method is mainly used in magnetostrictive Fe-based alloys (such as Fe–Ga alloys, Fe–Al alloys, etc.) with good plasticity and ductility, and the prepared magnetostrictive sheet materials exhibit relatively lower loss of eddy current in use [38,56]. At the same time, the rolling method has the advantages of high efficiency, low cost and obvious orientation [56,136,137]. But the stable forming and texture optimization is still an important issue in the production of magnetostrictive sheet materials by rolling method.

(3) Rapid quenching method

Rapid quenching method (Fig. 5 b) is a rapid cooling and non-equilibrium solidification method, and usually used to prepare magnetostrictive thin strips. Firstly, uniform as-cast alloys are obtained by vacuum non-consumable arc furnace melting. Samples less than 10 g are cut out from as-cast alloys and loaded into quartz glass tubes with 1 mm round holes at the bottom. The alloy is melted by induction heating to about 1300 °C in a vacuum strip-throwing furnace from quartz tips with argon or other inert gases. The nozzle sprays to the surface of the copper roll rotating at a high speed. The melt cools instantly and solidifies rapidly after contacting the roll surface and the melt sprays forward to form a thin strip by the centrifugal force of roll rotation. During the

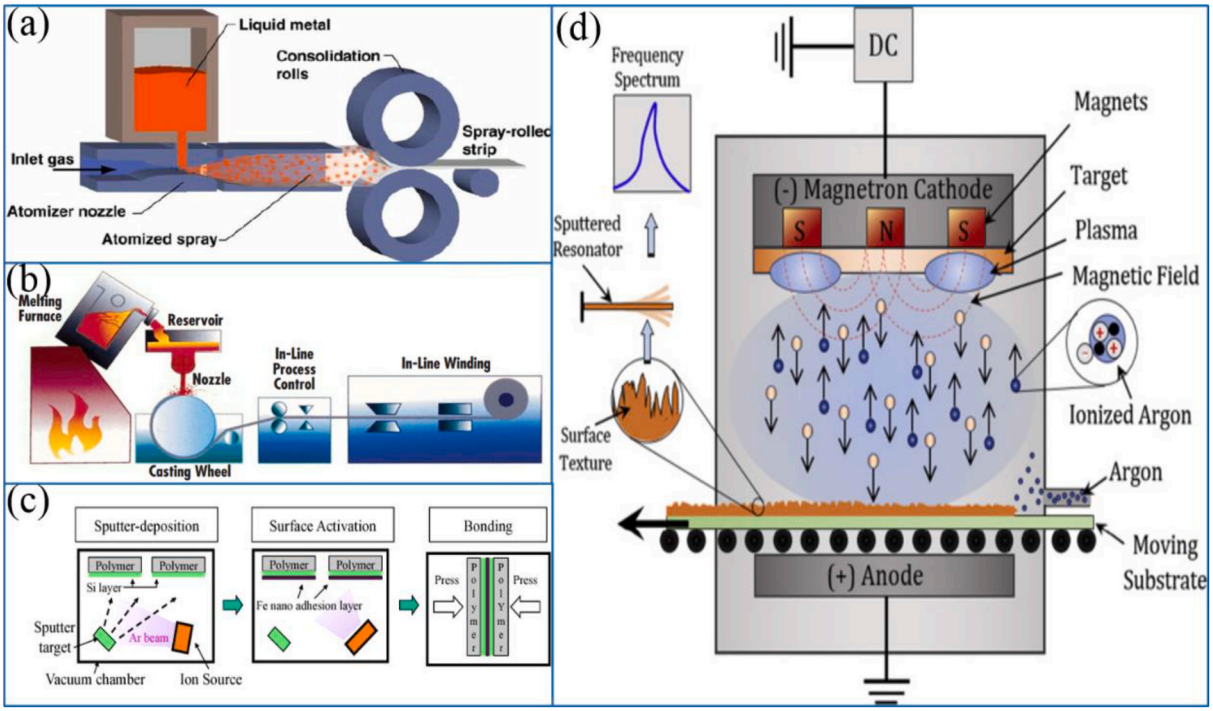

Fig. 5. Schematic setups for (a) rolling method, Reproduced with permission from Ref. [135] Copyright 2020 Springerlink, (b) rapid quenching method, (c) bonding method, Reproduced with permission from Ref. [147] Copyright 2015 IOPscience, (d) magnetron sputtering method [148].

process of extreme solidification of the thin strip, there are large stress gradients and temperature gradients on the free surface and the roll surface. Consequently, columnar crystals with orientation <l00> can be formed and make an important contribution to the large magnetostriction [38,138]. Some rare earth-based and Fe-based materials are commonly prepared by rapid quenching method. He et al. prepared FeGaPr alloy by using rapid quenching method and the magnetostrictive coefficient of the alloy reached −800 ppm, which was far higher than that obtained by conventional as-cast method [139,140].

(4) Bonding method

Bonding method (Fig. 5 c) appeared in the 1970s and refers to the process of mixing alloy powders, which are smelted and grinded by electric arc furnace, with binders such as resin plastics or alloys with low melting points, and then pressing, extrusion or injection moulding to form composite materials of a certain shape [141]. Although the addition of binders may cause the change of material composition, as well as the density and magnetic properties of the material [142], the bonding method has the advantages of simple process, high utilization of raw materials, and low cost. And magnetostrictive materials with complex shape can be prepared by using bonding method. At the same time, both the resistance and the high frequency characteristics of the magnetostrictive materials can be improved by the binders [143].

(5) Magnetron sputtering method

Magnetron sputtering (Fig. 5 d) is a method of filling argon in high vacuum, applying several hundred V DC voltages between cathode and anode, and producing magnetically controlled abnormal glow discharge in coating chamber, which ionizes argon. It is capable of growing films at low temperature and the films obtained by magnetron sputtering have the advantages of strong adhesion and low saturated magnetic field [144,145]. Allenstein et al. take the advantages of magnetron sputtering method to fabricate binary Fe–Pd submicron structures for biological applications which showed good biological properties [146]. However, it is necessary to make the films more compact and uniform in order to improve the thermal sensitivity and mechanical properties of the films.

In summary, it can be seen that the main efforts have been devoted to developing the preparation methods that can obtain large magnetostrictive strains. To date, most of the developed preparation methods, including rolling method, rapid quenching method, and magnetron sputtering method, etc., commonly oriented for the preparation of thin sheet magnetostrictive materials. In comparison, bonding method is suitable for the preparation of composite magnetostrictive materials with complex shape while directional solidification method is more suitable for the preparation of large-sized magnetostrictive materials. One of the future research emphases should be put on exploring the preparation and applications of magnetostrictive materials with both large-sized dimensions and excellent magnetostrictive properties.

4.2. Measurement methods

Measurement methods of magnetostriction can be broadly divided into direct measurement methods and indirect measurement methods, depending on whether the strain is measured directly or deduced from other parameters related to the strain [149].

(1) Direct measurements methods

Strain gauge method measures magnetostriction by measuring the resistance change of strain sensor, which is converted by the magnetostriction-induced deformation. This method has the advantages of stable performance, high sensitivity and low price [150]. A typical setup for strain gauge method is shown in Fig. 6 a [72]. It is a method of transforming magnetostrictive deformation into resistivity change by using strain gauge. When the sample deforms, the resistance value of strain gauge changes accordingly, and the magnetostrictive strain λ_s of the sample can be expressed as: $\lambda_s = \frac{\Delta l}{l} = CK\frac{\Delta R}{R}$, in which C is the structural parameter of strain resistor, R is the original value of strain resistor, K is the magnification of measurement system [151].

The strain changes of magnetostrictive materials are in the magnitude of ppm under the action of magnetic field, which requires very high sensitivity of the measurement methods. The capacitance dilatometry method (Fig. 6 b) is capable for measuring small macroscopic changes in solids and is known for its high sensitivity [152]. White et al. firstly

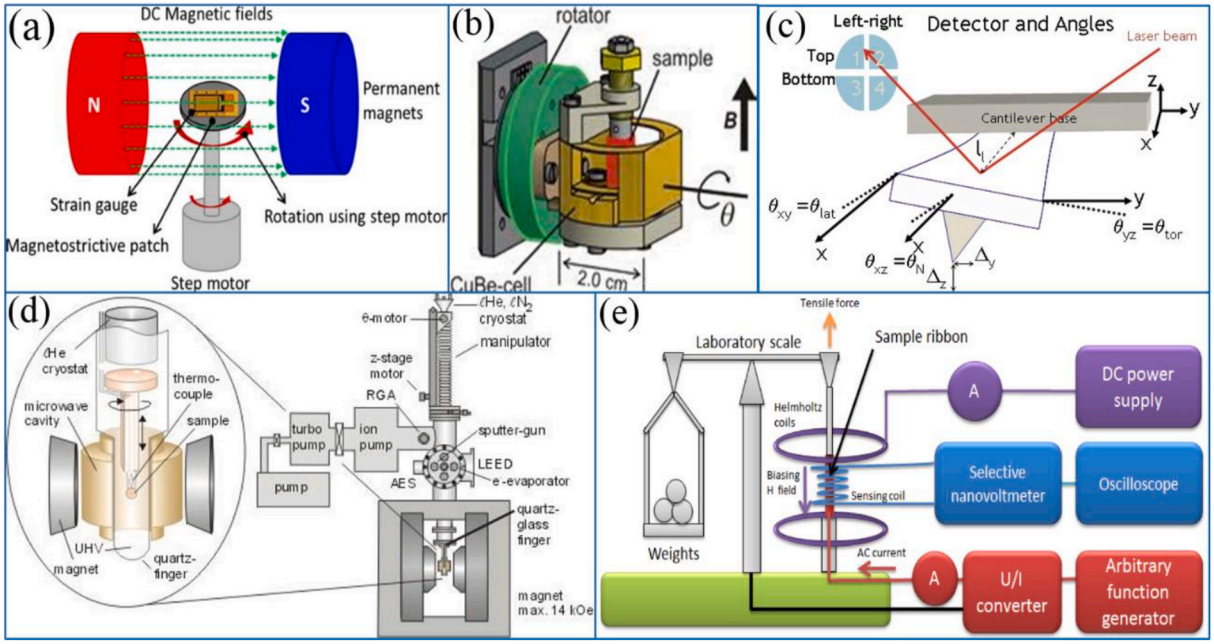

Fig. 6. Measurement methods of magnetostriction: (a) strain gauge method. Reproduced with permission from Ref. [72] Copyright 2014 IOPscience, (b) capacitance dilatometry method. Reproduced with permission from Ref. [152] Copyright 2012 AIP, (c) synergetic measurement method by optical- and mechanical-levers, (d) strain modulated ferromagnetic resonance, (e) Small-angle magnetization rotation. Reproduced with permission from Ref. [160] Copyright 2019 MDPI.

developed a three-terminal capacitance dilatometer for magnetostrictive measurement in 1961 [153]. Nowadays, three-terminal capacitance bridges provide a high-resolution measurement approach for magnetostriction with a precision of 10^{-9} in static fields up to 45 T and in pulse fields up to 60 T [154].

It is a simple method to measure magnetostriction by traditional optical method, in which the excitation magnetic field is generated by solenoid and the magnification measurement of micro-displacement is realized by the combination of mechanical lever and optical lever (Fig. 6 c) [155]. A superiority of this method is that there is no contact between the probe and the sample during the measurement [156]. However, this method has limited measurement accuracy and is only applicable for materials with relatively large dimensions.

(2) Indirect measurements methods

In 1865, Villari discovered that when iron was magnetized in a magnetic field, its magnetization curve varied with the stress after applying a small amount of stress. Villari effect is the inverse effect of Joule effect and sparks the exploration of indirect measurement methods of magnetostriction, which involve no direct measurements of the dimension change [157].

In strain modulated ferromagnetic resonance method (Fig. 6 d), the signal height obtained by phase-sensitive detection is proportional to the depth of strain modulation. By comparing the height of the strain modulated ferromagnetic resonance signal with the height of the ferromagnetic resonance line, the corresponding magnetostrictive strain can be obtained. This method has the advantages of high sensitivity, wide temperature range, and suitable for thin sheet materials.

The small-angle magnetization rotation method (Fig. 6 e) is an ideal method for measuring the magnetostriction of amorphous materials [158]. In this method, a static saturate magnetic field (bias field) is applied on the axial direction of sample. Then, a small AC magnetic field (driving field) is applied transversely by a solenoid. In this way, the saturation magnetization of the sample would be rotated lengthwise by a small angle, which can be converted into the induced voltage in the sensing coil around the sample. This method is suitable for measuring small magnetostriction and the magnetostriction of filamentous materials [159].

5. Biological performance and applications of magnetostrictive alloys

Biomedical science is a subject that uses the principles and methods of modern natural science and engineering technology to study the structure and function of human body and other life phenomena from the perspective of engineering. Biomedical applications mainly include biomedical measurement and monitoring, biomedical information processing, biomedical treatment, and so on. The different properties of biomaterials play a crucial role in the aforementioned biomedical applications. On all account, these materials should have good biocompatibility, such as histocompatibility, hemocompatibility, etc., without toxicity, and would not induce immunological rejections or inflammatory responses. In addition, biomaterials should also be sensitive to electrical, magnetic, or mechanical signals for biomedical measurement and monitoring as well as biomedical information processing. For biomedical treatment, specific therapeutical effects, certain mechanical properties and biological aging resistance are usually necessary. On this basis, magnetostrictive materials have aroused considerable interest in biomedical applications due to their special properties. For example, they are commonly used as physical sensors for temperature, pressure, liquid viscosity and flow velocity, and as chemical sensors for pH, carbon dioxide [161]. Therefore, many studies have focused on the biological properties of magnetostrictive alloys, including the cellular behavior and mechanisms of magnetostriction, as well as the latest applications of magnetostrictive alloys in remote cell drive, magnetic field sensor and wireless implantable device.

5.1. Cellular behavior

5.1.1. Cell viability

Cell viability refers to the percentage of living cells in the total number of cells after co-culturing with biomaterials. Cell viability can be influenced by environmental factors, including parameters in cell culture, stimulations by drugs and growth factors, and responses to various diseases. The physiological state of cells can be obtained through the detection of cell viability and the common detection methods include 3-(4,5)-dimethylthiahiazo(z-y1)-3,5-di-phenytetrazoliumromide (MTT) method, 2,3-Bis-(2-methoxy-4-nitro-5-sulfophenyl) -2H-tetrazolium-5-carboxanilide (XTT) method, and so on. Vargas-Esteve et al. investigated the effects of Fe–Ga alloy films and microparticles on cell viability by using macrophages, osteoblasts and osteosarcoma cells [26]. The results showed that the Fe–Ga alloy films had no effects on the viability of the three kinds of cells, and no significant differences in cell activity were found after the Fe–Ga alloy microparticles entered the macrophages (Fig. 7 a and b). Holmes et al. described the application of three magnetostrictive materials, including $Fe_{88}Ga_{12}$, $Fe_{71}Ga_{29}$ and $Fe_{40}Ni_{38}Mo_4B_{18}$ alloys, as biodegradable implants [53]. Cytotoxicity results indicated that $Fe_{40}Ni_{38}Mo_4B_{18}$ alloy was not biocompatible while the degradation products of $Fe_{88}Ga_{12}$ and $Fe_{71}Ga_{29}$ alloys showed no adverse effects on the viability of L929 fibroblasts cells. Moreover, it was shown that the degradation rates of the magnetostrictive alloys could be controlled remotely by applying a magnetic field, which caused the magnetostrictive alloys to generate low-magnitude vibrations that hastened their degradation rates. Overall, they presented the great potential of magnetostrictive alloys as biodegradable, magnetically-controlled active implants. Other studies also showed that Fe–Pd alloy [162] and Tb-Dy-Fe alloy were non-toxic with or without external magnetic field, but Fe–Co alloy was shown to cause a significant decrease in cell viability within 24 h [163].

5.1.2. Cell proliferation

Cell proliferation is an important physiological function of living cells and an important life characteristic of organisms [164].Cells proliferate in the form of division. By means of cell division, unicellular organisms produce new individuals and multicellular organisms produce new cells to supplement the aging or dead cells. There are many methods to study cell proliferation, including bromodeoxyuridine (BrdU), 5-ethynyl-2′-deoxyuridine (EdU) and Cell Counting Kit-8 (CCK-8), etc., among which CCK-8 is the most common used method for cell proliferation assay. Wang et al. studied the in vitro cytocompatibility of three different types of Fe–Ga alloys, including $Fe_{81}Ga_{19}$, $(Fe_{81}Ga_{19})_{98}B_2$ and $(Fe_{81}Ga_{19})_{99.5}(TaC)_{0.5}$ alloys, as potential biodegradable metallic materials [165]. And MC3T3-E1 cells exhibited good adhesion and proliferation behavior on the surfaces of the Fe–Ga alloys after culture for 4 h and 24 h. Studies on ferrite showed that this ferromagnetic material had little effects on the proliferation behavior of cells and cells proliferated normally on the material surface [166], which was similar to that of Fe–Ga alloys [26]. Besides, a study on Terfenol-D/poly(vinylidene fluoride-co-trifluoroethylene) composite films also revealed no effects on cell proliferation, but further studies showed that the ability of cell proliferation was significantly improved after the application of an external magnetic field (Fig. 7 c and d) [67].

5.1.3. Cell morphology

Cell morphology is one of the most important factors in evaluating the biocompatibility of materials. There are many kinds of cell morphologies, such as sphere, polyhedron, spindle and cylinder and there is a close relationship between the morphologies and function of cells. Moreover, the physiological state of cells can also be evaluated from cell morphology. Scanning electron microscopy and fluorescence microscopy are usually used to characterize cell morphology [167,168]. In a

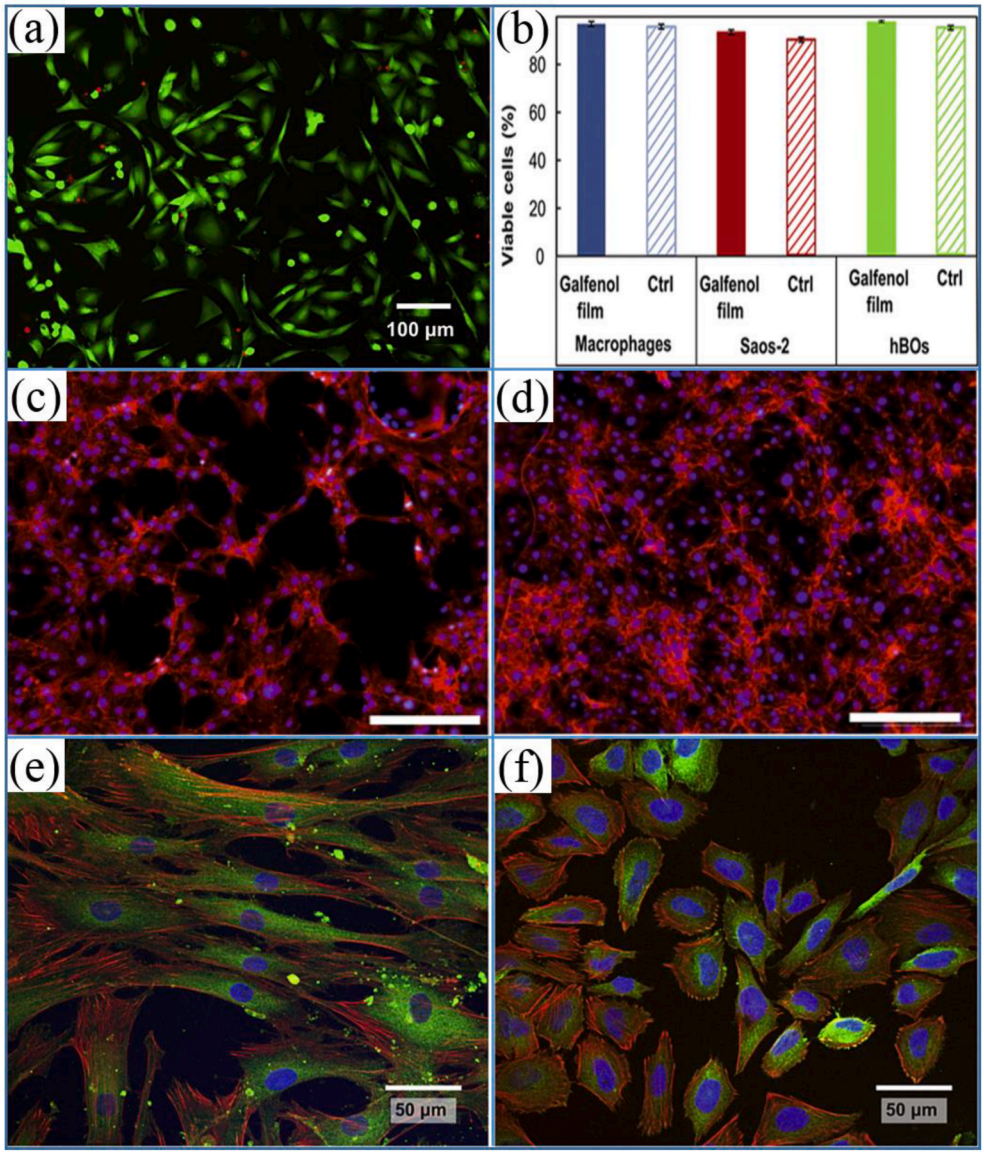

Fig. 7. (a) Live (green) and dead (red) Saos-2 cells and (b) percentage of viable macrophages, Saos-2 cells and hOBs growing on top of Fe–Ga alloy films or glass coverslips (Ctrl). Reproduced with permission from Ref. [26] Copyright 2017 Elsevier. Representative images of pre-osteoblast cultured after 72 h on Terfenol-D/poly(vinylidene fluoride-co-trifluoroethylene) composite films with (c) static and (d) dynamic conditions (nucleus stained with DAPI-blue and cytoskeleton stained with TRITC-red). Reproduced with permission from Ref. [67] Copyright 2016 Elsevier. Confocal laser scanning microscopy (CLSM) images of vinculin immunodetection (green), stress fibers distribution (red) and nuclei staining (blue) of (e) hOBs and (f) Saos-2 cells grown on Fe–Ga alloy films. Reproduced with permission from Ref. [26] Copyright 2017 Elsevier. (For interpretation of the references to colour in this figure legend, the reader is referred to the Web version of this article.)

study of Fe–Pd alloys, after culturing MG-63 cells together with the alloy extracts for 5 days, the cells exhibited a fusiform or polygonal shape with spike-like filopodia, indicating the normal growth of cells. Similar experiments were performed to explore the effect of ferrite on cell morphology, and the cultured Primary fetal human osteoblasts cells fHOb (406-05f) also showed typical polygonal or spindle morphology [169]. Moreover, when human osteoblast cells (hOBs) and human osteoblast-like cell line (Saos-2) were cultured on Fe–Ga alloy films, it was found that the two kinds of cells could establish focal contact with the alloy films and showed clear stress fiber profile, indicating good cell morphology (Fig. 7 e and f) [26].

5.2. Effect mechanisms of magnetostriction on cells

5.2.1. Mechanical stimulus induced by magnetostriction

According to the Joule effect and Villari effect, magnetostrictive materials can realize the conversion of magnetic energy and mechanical energy. Under the action of AC or direct current field, magnetostrictive materials can generate static or dynamic strain, thus resulting in mechanical stimulation. Since magnetostrictive strain is obtained by the function relation between the initial length of the material and the intensity of the applied magnetic field [161], the change of the corresponding strain can be remotely controlled by magnetic field. In addition, magnetostrictive strain is generally at the ppm level, so the resulting mechanical stimulation will hardly cause physical damage to cells. Therefore, magnetostrictive alloys are expected to play an important role in biomedical fields.

5.2.2. Effect mechanisms of mechanical stimulus on cells

Mechanical and chemical signals generated at cellular level have been shown to be closely related to the mutual mechanochemical transformation pathways (Fig. 8). Both intracellular forces (F_i) and externally applied forces (F_e) can produce mechanical signals that influence the function of cells (Fig. 8 a). F_i can be transferred to adjacent cells by intercellular junctions or the traction on extracellular matrix (ECM) adhesion ligands that are bound to integrin receptors. F_i in multiple cells can be coupled either directly through intercellular junctions or indirectly through solid forces applied to the ECM. F_e is usually applied to cells in the form of shearing, stretching, or compression. Cells can sense the changes of F_e through the deformations in cytoskeleton and primary cilium, the changes in receptor-ligand binding and mechanically gated ion channels. The cytoskeleton generates and transfers forces from membrane proteins to intracellular structures and influences cellular behavior through a series of

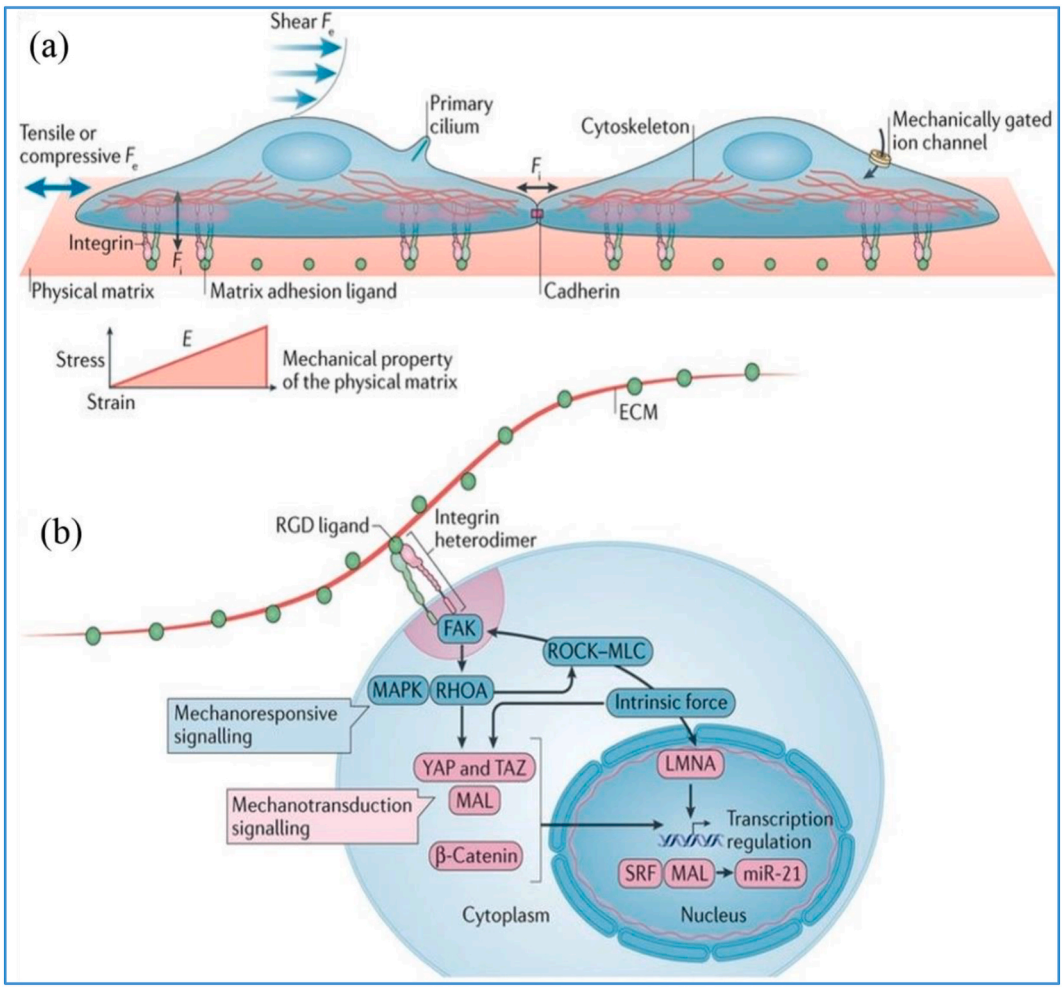

Fig. 8. (a) The action and transmission mode of F_i and F_e, (b) the transduction and transformation process of mechanochemical signals. Reproduced with permission from Ref. [170] Copyright 2017 Nature Reviews Molecular Cell Biology.

mechanochemical signal transduction and transformation (Fig. 8 b) [170].

Studies have shown that the proliferation and function of cells vary with different loading methods of mechanical stress. It was reported that strains below 200 ppm would not stimulate the remodeling of cortical bone in the human body [171]. Strains between 200 ppm and 2000 ppm represented the physiological strain level of human bones. Moreover, when strains exceeded 2000 ppm, the rate of bone formation is faster than that of bone absorption, leading to bone regeneration [172]. However, a study involving turkeys has shown that a strain signal with 30 Hz and 100 ppm was sufficient to maintain bone mass, and another study involving rats showed that a strain signal with 2 Hz and 930 ppm was sufficient to promote bone growth [173]. These results indicated that the cell response of mechanical stress depends on a combined action of various factors, including the loading types, magnitude, frequency and time of mechanical stress. And positive cell response can also be obtained with mechanical stress at relatively small magnitude if the loading frequency of mechanical stress is high enough [174].

5.3. Remote cell actuation

In recent years, magnetostrictive materials have aroused great interest for remote cell actuation in biomedical fields. Vargas-Estevez et al. explored the interactions between external magnetic field driven Fe–Ga alloy particles and cells. The alloy particles were cultured with macrophages and then entered the cells. After applying a static magnetic field, the chains of particles were generated on cell membrane and inside the cells. These chains could be controlled remotely through the magnetic field vector without affecting the cell morphology (Fig. 9 a and b) [26]. Ribeiro et al. cultured MC3T3-E1 pre-osteoblast cells on Terfenol-D/poly(vinylidene fluoride-co-trifluoroethylene) composite films, and a remote controlled magnetic field was applied to generate mechanical stimulation (up to 110 ppm) during the culture process (Fig. 9 c and d) [67]. It was found that the mechanical stimulation increased the number of osteoblasts by about 20%, indicating the impressive capability of magnetostriction in remote cell actuation. Furthermore, Hart et al. directly bonded Terfenol-D composites to a pig tibia, and applied an external magnetic field of 30 Hz and 170 kA/m. A strain of more than 900 ppm was detected on the bone surface and demonstrated the effectiveness of Terfenol-D composites to stimulate bone tissue formation via remote magnetostrictive actuation (Fig. 9 e and f) [27].

5.4. Magnetic field sensors

Magnetostrictive materials can be used to manufacture special magnetic field sensors for biological magnetic field measurement. The measurement of biological magnetic field is an effective noninvasive method for clinical detection, such as using magnetoencephalography (MEG) and magnetocardiography (MCG) to study human advanced brain function [175]. The measurement of biological magnetic field requires the sensor to have a low detection limit in the low frequency

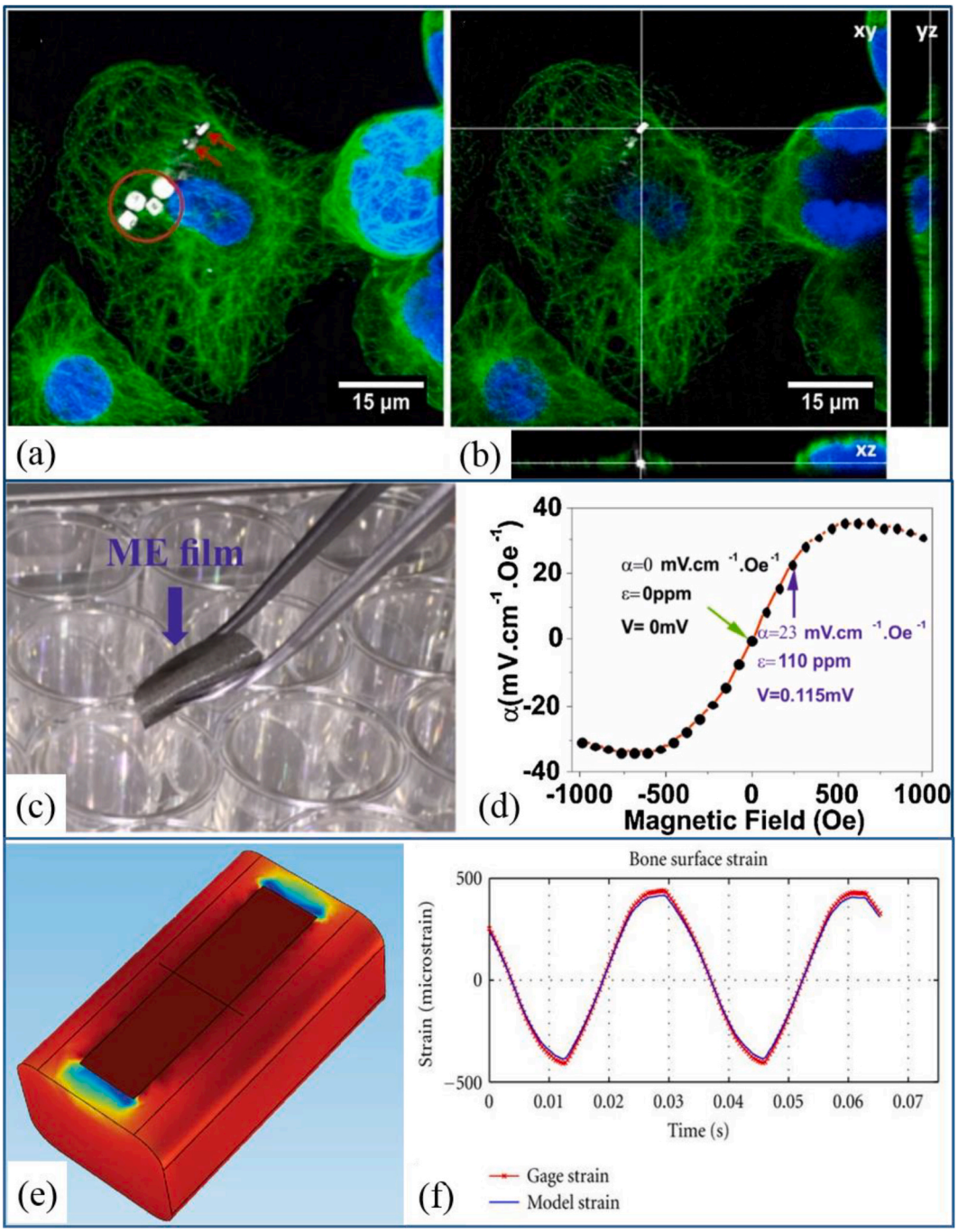

Fig. 9. The interaction between macrophage cytoskeleton and Galfenol-based microparticles after magnetic exposure. (a) CLSM reconstructed 3D and (b) orthogonal image of the same macrophages exposed to the magnetic field for 1 min and cultured for 24 h. One of the macrophages showed 6 Fe–Ga alloy microparticles, 4 of which inside the red circle and 2 of which pointed by red arrows. Orthogonal projection showed that at least two of these microparticles were inside the cell (yz image (right) and zx image (bottom)). Microtubules stained in green showed a normal distribution. Nuclei stained with Hoechst were in blue and microparticles visualized by reflection were seen in white. Reproduced with permission from Ref. [26] Copyright 2017 Elsevier. (c) Terfenol-D/poly(vinylidene fluoride-co-trifluoroethylene) film and (d) corresponding magnetoelastic characterization with α (magnetoelastic coefficient), strain (ε) and voltage (V) values that will be generated during the dynamic cell culture. Reproduced with permission from Ref. [67]. Copyright 2017 Elsevier. After bonding Terfenol-D composite to a bone and driven at 30 Hz and 170 kA/m: (e) the strain distribution along longitudinal direction of bone model by finite element analysis, (f) predicted strain from the model versus gage strain on the bone surface. Reproduced with permission from Ref. [27] Copyright 2012 Smart Materials Research. (For interpretation of the references to colour in this figure legend, the reader is referred to the Web version of this article.)

range [176]. The amorphous soft magnetic alloys FeGaB and FeCoSiB have been developed as magnetic field sensors for biological magnetic field measurement due to their high magnetostriction and high permeability [177]. Yu et al. developed a MEMS resonant magnetic field sensor based on AlN/FeGaB bilayer nano plate resonator (Fig. 10 a), which shows a frequency sensitivity of ~1 Hz/nT and a detection limit of ~10 nT [60]. Reermann et al. evaluated a thin-film magnetoelectric (ME) sensor for measuring R-waves in human heart (Fig. 10 b). Taking advantage of the magnetostrictive properties of FeCoSiB, an exchange bias stack based on 20 times 5 nm Ta/3 nm Cu/8 nm MnIr/200 nm FeCoSiB was sputtered on the bottom side to improve the sensitivity of the sensor [178]. Moreover, Ren et al. made use of the special properties

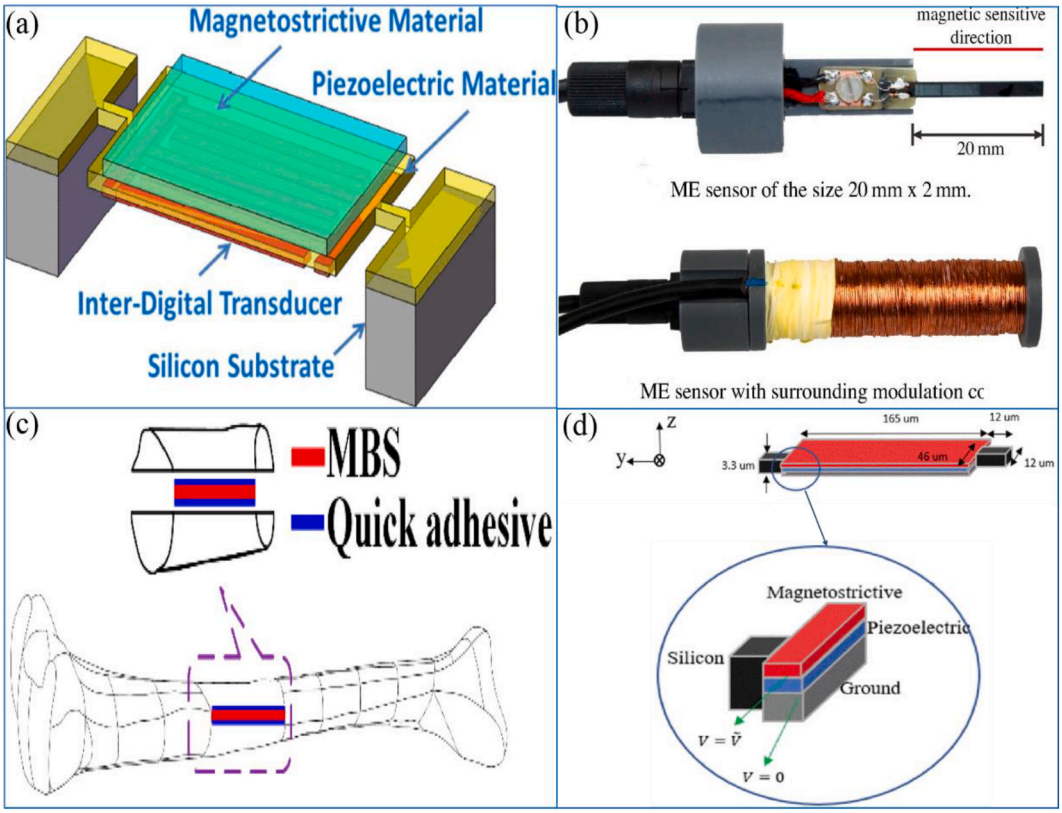

Fig. 10. The applications of magnetostrictive materials in biomagnetic field measurement and wireless implantable devices. (a) 3D schematic of the MEMS resonant magnetic field sensor based on AlN/FeGaB bilayer nanoplate resonator. Reproduced with permission from Ref. [60] Copyright 2013 IEEE. (b) The ME sensor used for measuring R-waves in human heart. Reproduced with permission from Ref. [178] Copyright 2018 Elsevier. (c) Model for monitoring and evaluating the degradation rate of artificial bone and MBS refers to magnetoelastic-based sensor. Reproduced with permission from Ref. [179] Copyright 2018 MDPI. (d) ME heterostructure consisting of a piezoelectric AlN film and a magnetostrictive FeGaB film. Reproduced with permission from Ref. [182] Copyright 2020 IEEE.

of magnetostrictive materials to develop wireless magnetoelastic sensors that can monitor and evaluate the degradation rate of artificial bone in vitro (Fig. 10 c) [179]. These results indicate the great potential of magnetostrictive materials in improving the detection ability of magnetic sensors for biomagnetic field measurements.

5.5. *Wireless implantable devices*

Conventional electromagnetic based wireless implants are usually limited by their oversized antennas [180,181]. In comparison, the ME antenna made of piezoelectric material bonded by magnetostrictive layer can be miniaturized without causing significant performance degradation. Rangriz et al. simulated a ME heterostructural antenna consisting of a piezoelectric AlN film and a magnetostrictive FeGaB film for wireless link applications (Fig. 10 d). The results showed that the ME antenna had the advantages of low loss, high matching and high efficiency when used as an implantable devices [182]. In addition, Zaeimbashi et al. developed a novel, wireless, ultra-compact brain implantable device termed NanoNeuroRFID which used a ME antenna of the same structure with the one developed by Rangriz et al. This device can realize self-power supply, contactless induction of neural magnetic fields, communication with external transceivers and other functions [172]. In a word, magnetostrictive materials have shown great potential to be used in wireless implantable devices to effectively improve their performance.

6. Conclusions and prospects

Magnetostriction phenomenon has become a hot research topic in various fields. In this work, recent studies on magnetostrictive alloys have been reviewed with a focus on biomedical applications. A comparatively perfect theoretical system, including microscopic theory, has laid a solid theoretical foundation for the development of magnetostriction. In addition, researchers have developed a variety of magnetostrictive materials. Among them, rare earth based alloys with giant magnetostriction are the most widely used magnetostrictive materials at present, while the newly emerged Fe–Ga alloys are gaining increasing attention owing to their good machinability and high magnetostrictive strain under low magnetic field. Moreover, many preparation methods have been developed for magnetostrictive materials with different properties, such as the directional solidification method for the preparation of large-size block materials, the rapid quenching method for the preparation of thin film materials, etc. The diversity of preparation methods provides convenience for the preparation of magnetostrictive materials used in different occasions. On the other hand, it has always been challenging to explore the accurate measurement of magnetostriction. Magnetostriction is commonly measured by direct methods, in which strain gauge method is one of the mostly used methods while capacitance dilatometry has relatively higher sensitivity. Recently, the developed indirect measurement methods provide an alternative for the precise measurement of magnetostriction. Furthermore, most magnetostrictive alloys have been shown to be biocompatible, and magnetostriction is capable of providing mechanical stimulation by remote regulation, which opens up new potential directions for magnetostriction in regulating cellular behavior and various biomedical applications.

However, there are still several challenges of magnetostriction for biomedical applications. (1) The in vitro and in vivo biocompatibility of magnetostrictive materials should be systematically studied for biosafety. Moreover, the existing magnetostrictive materials applicable

for biomedical applications are still scarce, for example, Terfenol-D has good magnetostrictive properties but limited machinability and potential biotoxicity due to the high level of rare earth elements, while Fe–Ga alloys have shown good extracellular and intracellular response but their saturated magnetostriction are limited for providing effective mechanical stimulation. Therefore, more efforts should be devoted to developing magnetostrictive materials with both good magnetostriction and biocompatibility. (2) Novel methods should be developed for the 3D preparation and accurate measurement of magnetostrictive materials with potential complex shape and internal structure. (3) Further studies are needed in the precise regulation of magnetostriction for biomedical applications. (4) Studies on the interactions between magnetostrictive materials and cells/tissues are still in infancy. Anyway, it is a promising direction worthy of future research to apply the reciprocating strain characteristics of magnetostrictive materials in remote cell regulation and magnetostriction is expected to achieve more breakthroughs and applications in biomedical fields.

Ethical approval

This study does not contain any studies with human or animal subjects performed by any of the authors.

Conflict of interest

The authors declare that they have no conflict of interest.

Acknowledgment

This study was supported by the following funds: (1) The Natural Science Foundation of China (51935014, 82072084, 81871498); (2) Hunan Provincial Natural Science Foundation of China (2020JJ3047, 2019JJ50588); (3) The Provincial Key R & D Projects of Jiangxi (20201BBE51012); (4) JiangXi Provincial Natural Science Foundation of China (20192ACB20005); (5) National Engineering Research Center of Near-Net-Shape Forming for Metallic Materials Open Fund, SCUT (2020004); (6) Guangdong Province Higher Vocational Colleges & Schools Pearl River Scholar Funded Scheme (2018); (7) Innovation Team Project on University of Guangdong Province (2018GKCXTD001); (8) Technology Innovation Platform Project of Shenzhen Institute of Information Technology (PT2020E002).

References

[1] You-li Han, Evolution of the concept of health and enlightenment on healthcare reform, Chin. Med. Ethics 24 (1) (2011).
[2] D.H. Hu, K. Tao, To see the future development of burn medicine from the view of holistic integrative medicine, Zhonghua shao shang za zhi= Zhonghua shaoshang zazhi= Chin. J. burns 33 (4) (2017) 193–195.
[3] Kaoru Funaki, Hidenobu Fukunishi, Tsuyoshi Funaki, Katsuhiro Sawada, Yasushi Kaji, Takeshi Maruo, Magnetic resonance-guided focused ultrasound surgery for uterine fibroids: relationship between the therapeutic effects and signal intensity of preexisting T2-weighted magnetic resonance images, Am. J. Obstet. Gynecol. 196 (2) (2007) 184. e1–184. e6.
[4] Pingsheng Fan, Tengyue Zhang, Qiang Huang, Wei Qiang, Xin Sun, Liting Qian, Basic and clinical research on the therapeutic effect of intervention in primary liver cancer by targeted intra-arterial verapamil infusion, Cell Biochem. Biophys. 62 (1) (2012) 59–67.
[5] Xia Chen, Jian Wang, Li Yu, Zhou Jia, Danning Zheng, Bo Zhang, Effect of concentrated growth factor (CGF) on the promotion of osteogenesis in bone marrow stromal cells (BMSC) in vivo, Sci. Rep. 8 (1) (2018) 1–8.
[6] Fangwei Qi, Chen Wang, Shuping Peng, Cijun Shuai, Wenjing Yang, Zhenyu Zhao, A co-dispersed nanosystem of strontium-anchored reduced graphene oxide to enhance the bioactivity and mechanical property of polymer scaffolds, Mater. Chem. Front. 5 (5) (2021) 2373–2386.
[7] K.H. Fuchs, Minimally invasive surgery, Endoscopy 34 (2) (2002) 154–159.
[8] F. Cepolina, R.C. Michelini, Review of robotic fixtures for minimally invasive surgery, Int. J. Med. Robot. Comput. Assist. Surg. 1 (1) (2004) 43–63.
[9] Laura Curiel, Francoise Chavrier, Rémi Souchon, Alain Birer, Jean Y. Chapelon, 1.5-D high intensity focused ultrasound array for non-invasive prostate cancer surgery, IEEE Trans. Ultrason. Ferroelectrics Freq. Contr. 49 (2) (2002) 231–242.
[10] Sunita Chauhan, R. Mishra, S. Kumar, M.Y. Teo, A Robot for Non-invasive Breast Cancer Surgery, 7th International Conference on Control, Automation, Robotics and Vision, 2002. ICARCV 2002, IEEE, 2002, pp. 425–428.
[11] Sunita Chauhan, Gerald Gim Lee Seet, Hybrid Supervisory Control for Biomechatronic Systems for Non-invasive Surgery, Solid State Phenomena, Trans Tech Publ, 2009, pp. 251–257.
[12] Safdar N. Khan, Frank P. Cammisa Jr., S Sandhu Harvinder, Ashish D. Diwan, Federico P. Girardi, Joseph M. Lane, The biology of bone grafting, JAAOS 13 (1) (2005) 77–86.
[13] Mark H. Hofbauer, Rick J. Delmonte, Mark L. Scripps, Autogenous bone grafting, J. Foot Ankle Surg. 35 (5) (1996) 386–390.
[14] Vittorio Moraschini, Almeida Daniel Costa Ferreira de, Monica Diuana Calasans-Maia, Ingrid Chaves Cavalcante Kischinhevsky, Rafael Seabra Louro, José Mauro Granjeiro, Immunological response of allogeneic bone grafting: a systematic review of prospective studies, J. Oral Pathol. Med. 49 (5) (2020) 395–403.
[15] Masataka Deie, Mitsuo Ochi, Nobuo Adachi, Makoto Nishimori, Kazunori Yokota, Artificial bone grafting [calcium hydroxyapatite ceramic with an interconnected porous structure (IP-CHA)] and core decompression for spontaneous osteonecrosis of the femoral condyle in the knee, Knee Surg. Sports Traumatol. Arthrosc. 16 (8) (2008) 753–758.
[16] Youwen Yang, Yun Cheng, Fang Deng, Lida Shen, Cijun Shuai, A Bifunctional Bone Scaffold Combines Osteogenesis and Antibacterial Activity via in Situ Grown Hydroxyapatite and Silver Nanoparticles, Bio-Design and Manufacturing, 2021.
[17] Guowen Qian, Lemin Zhang, Guoyong Wang, Zhengyu Zhao, Shuping Peng, Cijun Shuai, 3D printed Zn-doped mesoporous silica-incorporated poly-L-lactic acid scaffolds for bone repair, Int. J. Bioprint. 7 (2) (2021) 346.
[18] Shekhar Bhansali, Abhay Vasudev, MEMS for Biomedical Applications, Elsevier, 2012.
[19] Hong-sheng Hu, Guang-feng Wu, Wen-jian Zhu, The application and development of the area that the MEMS are used in the biomedical field [J], Mod. Manuf. Eng. 9 (2007).
[20] Clarisse Ribeiro, Vítor Sencadas, Daniela M. Correia, Senentxu Lanceros-Méndez, Piezoelectric polymers as biomaterials for tissue engineering applications, Colloids Surf. B Biointerfaces 136 (2015) 46–55.
[21] Debashish Roy, Jennifer N. Cambre, Brent S. Sumerlin, Future perspectives and recent advances in stimuli-responsive materials, Prog. Polym. Sci. 35 (1–2) (2010) 278–301.
[22] Cijun Shuai, Bo Peng, Feng Pei, Li Yu, Ruilin Lai, Anjie Min, in situ synthesis of hydroxyapatite nanorods on graphene oxide nanosheets and their reinforcement in biopolymer scaffold, J. Adv. Res. 16 (2021).
[23] Carolina De las Heras Alarcón, Sivanand Pennadam, Cameron Alexander, Stimuli responsive polymers for biomedical applications, Chem. Soc. Rev. 34 (3) (2005) 276–285.
[24] Marcelo J. Dapino, On magnetostrictive materials and their use in smart material transducers, Struct. Eng. Mech. J 17 (2002) 1–28.
[25] T. Klinger, H. Pfutzner, P. Schonhuber, K. Hoffmann, N Bachl, Magnetostrictive amorphous sensor for biomedical monitoring, IEEE Trans. Magn. 28 (5) (1992) 2400–2402.
[26] Carolina Vargas-Estevez, Andreu Blanquer, Prabesh Dulal, Rafael Pérez Del Real, Marta Duch, Ibáñez Elena, Leonardo Barrios, Gonzalo Murillo, Núria Torras, Carme Nogués, Study of Galfenol direct cytotoxicity and remote microactuation in cells, Biomaterials 139 (2017) 67–74.
[27] Stephen Hart, Bucio Ryan, Marcelo Dapino, Magnetostrictive actuation of a bone loading composite for accelerated tissue formation, Smart Mater. Res. 2012 (2012).
[28] James Prescott Joule, On a new class of magnetic forces, Ann. Electr. Magn. Chem 8 (1842) 219–224.
[29] E. Villari, Intorno alle modificazioni del memento magnetico di una verga di ferro e di acciaio, prodotte per la trazione della medesima e pel passaggio di una corrente attraverso la stessa, Il Nuovo Cimento 20 (1) (1864) 317–362.
[30] Evangelos Hristoforou, Aphrodite Ktena, Magnetostriction and magnetostrictive materials for sensing applications, J. Magn. Magn Mater. 316 (2) (2007) 372–378.
[31] Ruben Decocker, Leo Kestens, Yvan Houbaert, Modelling the magnetostriction coefficient of polycrystalline ferromagnetic materials with a cubic structure by means of the finite element method, J. Magn. Magn Mater. 242 (2002) 1218–1220.
[32] Wenxian Li, Yu Kun, Din Cheng, Super magnetostrictive material of rare-earths–a study, Min. Metall. Eng. 20 (3) (2000) 64–67.
[33] L. Pîslaru-Dănescu, Alexandru M. Morega, Mihaela Morega, A novel magnetostrictive injection actuator based on new giant magnetostrictive materials, in: 7th International Symposium on Advanced Topics in Electrical Engineering (ATEE), IEEE, 2011, pp. 1–6.
[34] Yoon Young Kim, Young Eui Kwon, Review of magnetostrictive patch transducers and applications in ultrasonic nondestructive testing of waveguides, Ultrasonics 62 (2015) 3–19.
[35] Marcelo J. Dapino, On magnetostrictive materials and their use in adaptive structures, Struct. Eng. Mech. 17 (3–4) (2004) 303–330.
[36] Jiquan Wang, Anisotropy and Magnetostriction of Cobalt Ferrite, University of Science and Technology Beijing, 2018.
[37] M. Fähnle, T. Egami, Phenomenological theory of magnetostriction in amorphous ferromagnets, J. Appl. Phys. 53 (3) (1982) 2319–2320.
[38] Guangrui Zhang, Microstructure and Properties of Fe-Ga-Tb Magnetostrictive Alloy, hebei university of technology, 2015.
[39] Yu Zhang, Fabrication of Fe-Ga Magnetostrictive Alloy and Study on La, Ce Rare Earth Doping, Xihua University, 2017.

[40] Man-Gui Han, Long-Jiang Deng, Mössbauer studies on the shape effect of Fe84.94Si9.68Al5.38 particles on their microwave permeability, Chin. Phys. B 22 (8) (2013), 083303.
[41] James R. Cullen, Arthur E. Clark, Magnetostriction and structural distortion in rare-earth intermetallics, Phys. Rev. B 15 (9) (1977) 4510.
[42] L. Bumagina, V. Krotov, B. Malkin, A Kh Khasanov, Magnetostriction in ionic rare earth paramagnets, Zh. Eksp. Teor. Fiz. 80 (1981) 1543–1553.
[43] H. Hasegawa, A theory of magneto-volume effects of itinerant-electron magnets. I. Spontaneous volume magnetostriction, J. Phys. C Solid State Phys. 14 (20) (1981) 2793.
[44] P.P.M. Meincke, Calculation of the magnetostriction and thermal expansion of an itinerant-electron ferromagnet, Can. J. Phys. 48 (7) (1970) 859–861.
[45] I.C. Nlebedim, J.E. Snyder, A.J. Moses, D.C. Jiles, Anisotropy and magnetostriction in non-stoichiometric cobalt ferrite, IEEE Trans. Magn. 48 (11) (2012) 3084–3087.
[46] Yoshio Suzuki, Norio Ohta, Single ion model for magnetostriction in rare-earth–transition-metal amorphous films, J. Appl. Phys. 63 (8) (1988) 3633–3635.
[47] Jinghua Liu, Chengbao Jiang, Huibin Xu, Giant magnetostrictive materials, Sci. China Technol. Sci. 55 (5) (2012) 1319–1326.
[48] Xuegen Zhao, Nigel Mellors, D.G. Lord, Magnetomechanical performance of directionally solidified Fe–Ga alloys, J. Appl. Phys. 101 (9) (2007), 09C513.
[49] P. Taheri, R. Barua, J. Hsu, M. Zamanpour, Y. Chen, V.G. Harris, Structure, magnetism, and magnetostrictive properties of mechanically alloyed Fe81Ga19, J. Alloys Compd. 661 (2016) 306–311.
[50] D.C. Jiles, Recent advances and future directions in magnetic materials, Acta Mater. 51 (19) (2003) 5907–5939.
[51] M. Leonowicz, Magnetostrictive materials, Inzynieria Mater. 25 (2) (2004) 68–70.
[52] T Toby Hansen, Magnetostrictive materials and ultrasonics, Chemtech 26 (8) (1996) 56–59.
[53] Hal R. Holmes, Andrew DeRouin, Samantha Wright, M Riedemann Travor, Thomas A. Lograsso, Rupak M. Rajachar, Keat Ghee Ong, Biodegradation and biocompatibility of mechanically active magnetoelastic materials, Smart Mater. Struct. 23 (9) (2014), 095036.
[54] Qingsong Xing, Y. Du, R.J. McQueeney, T.A. Lograsso, Structural investigations of Fe–Ga alloys: phase relations and magnetostrictive behavior, Acta Mater. 56 (16) (2008) 4536–4546.
[55] R. Grössinger, R. Sato Turtelli, N. Mehmood, S. Heiss, H. Müller, C. Bormio-Nunes, Giant magnetostriction in rapidly quenched Fe–Ga, J. Magn. Magn Mater. 320 (20) (2008) 2457–2465.
[56] Quan Fu, Yuhui Sha, Fang Zhang, Lei Fan, Liang Zuo, Strong Texture Development and Magnetostriction in Recrystallized Fe81Ga19 Thin Sheet, 2015 International Conference on Materials, Environmental and Biological Engineering, Atlantis Press, 2015, pp. 1055–1059.
[57] J.B. Restorff, M. Wun-Fogle, A.E. Clark, Thomas A. Lograsso, A.R. Ross, L Schlagel Deborah, Magnetostriction of ternary Fe–Ga–X alloys (X= Ni, Mo, Sn, Al), J. Appl. Phys. 91 (10) (2002) 8225–8227.
[58] Long-long Liao, Mei-ling Fang, Jie Zhu, Ji-heng Li, Jian Wang, Influence of Al on the magnetostriction of Fe-Ga polycrystal alloys under compressive stress, Int. J. Miner. Metall. Mater. 21 (1) (2014) 52–57.
[59] Yutian Ding, Chang Li, Guangzhu Liu, Yong Hu, Shankun Yu, Wang Jing, Effects of the ternary element(C,B) additions on phase constitution and magnetostriction of Fe_(83)Ga_(17) alloys, Mater. Rev. (2010).
[60] Yu Hui, T.X. Nan, N.X. Sun, Matteo Rinaldi, MEMS resonant magnetic field sensor based on an AlN/FeGaB bilayer nano-plate resonator, in: IEEE 26th International Conference on Micro Electro Mechanical Systems (MEMS), IEEE, 2013, pp. 721–724.
[61] Tingyan Jin, Wei Wu, Chengbao Jiang, Improved magnetostriction of Dy-doped Fe83Ga17 melt-spun ribbons, Scripta Mater. 74 (2014) 100–103.
[62] Tetsuroh Kawai, Tatsuya Abe, Mitsuru Ohtake, Masaaki Futamoto, Magnetostrictive behaviors of Fe-Al (001) single-crystal films under rotating magnetic fields, AIP Adv. 6 (5) (2016), 055931.
[63] Shin-ichi Yamaura, Microstructure and magnetostriction of heavily groove-rolled Fe-Co alloy wires, Mater. Sci. Eng., B 264 (2021) 114946.
[64] Shuai Ren, Dezhen Xue, Yuanchao Ji, Xiaolian Liu, Sen Yang, Xiaobing Ren, Low-field-triggered large magnetostriction in iron-palladium strain glass alloys, Phys. Rev. Lett. 119 (12) (2017) 125701.
[65] Yin Liu, Qiang Wang, Tie Liu, Pengfei Gao, Yi Yuan, Jicheng He, Effects of high magnetic fields on the crystal orientation and magnetostriction of a TbFe2 based alloy during treatment in the semi-solid state, J. Alloys Compd. 590 (2014) 110–115.
[66] Xiaoyu Guo, Meng Dong, Tie Liu, Yubao Xiao, Shuang Yuan, Qiang Wang, Magnetic Domain and Magnetic Properties of Tb-Dy-Fe Alloys Directionally Solidified and Heat Treated in High Magnetic Fields, IEEE Transactions on Magnetics, 2020.
[67] Clarisse Ribeiro, V. Correia, P. Martins, F.M. Gama, S. Lanceros-Mendez, Proving the suitability of magnetoelectric stimuli for tissue engineering applications, Colloids Surf. B Biointerfaces 140 (2016) 430–436.
[68] S.D. Bhame, P.A. Joy, Enhanced magnetostrictive properties of CoFe2O4 synthesized by an autocombustion method, Sensor Actuator Phys. 137 (2) (2007) 256–261.
[69] W. Jahjah, R. Manach, Y. Le Grand, A. Fessant, B. Warot-Fonrose, A.R.E. Prinsloo, C.J. Sheppard, D.T. Dekadjevi, D. Spenato, J-Ph Jay, Thickness dependence of magnetization reversal and magnetostriction in Fe 81 Ga 19 thin films, Phys. Rev. Appl. 12 (2) (2019), 024020.
[70] Jayasimha Atulasimha, B Flatau Alison, A review of magnetostrictive iron–gallium alloys, Smart Mater. Struct. 20 (4) (2011), 043001.
[71] E.M. Summers, T.A. Lograsso, M. Wun-Fogle, Magnetostriction of binary and ternary Fe–Ga alloys, J. Mater. Sci. 42 (23) (2007) 9582–9594.
[72] Byungseok Yoo, Na Suok-Min, Alison B. Flatau, Darryll J. Pines, Directional magnetostrictive patch transducer based on Galfenol's anisotropic magnetostriction feature, Smart Mater. Struct. 23 (9) (2014), 095035.
[73] X. Zhao, N. Mellors, D.G. Lord, Magnetomechanical performance of directionally solidified Fe–Ga alloys, J. Appl. Phys. 101 (9) (2007), 09C513.
[74] R.A. Kellogg, A.M. Russell, T.A. Lograsso, A.B. Flatau, A.E. Clark, M. Wun-Fogle, Tensile properties of magnetostrictive iron–gallium alloys, Acta Mater. 52 (17) (2004) 5043–5050.
[75] Quanxia Hu, Dunbo Yu, Hongchuan Yang, Kuoshe Li, Development of magnetostrictive properties of Fe-Ga alloy, Chin. J. Rare Metals 1 (2013).
[76] Manfred Wuttig, Liyang Dai, James Cullen, Elasticity and magnetoelasticity of Fe–Ga solid solutions, Appl. Phys. Lett. 80 (7) (2002) 1135–1137.
[77] A.K. Mohamed, V.V. Palacheva, V.V. Cheverikin, E.N. Zanaeva, W.C. Cheng, V. Kulitckii, S. Divinski, G. Wilde, I.S. Golovin, The Fe–Ga phase diagram: Revisited, J. Alloys Compd. 846 (2020) 156–486.
[78] O. Ikeda, Ryosuke Kainuma, I. Ohnuma, K. Fukamichi, K. Ishida, Phase equilibria and stability of ordered bcc phases in the Fe-rich portion of the Fe–Ga system, J. Alloys Compd. 347 (1–2) (2002) 198–205.
[79] T.A. Lograsso, A.R. Ross, D.L. Schlagel, A.E. Clark, M. Wun-Fogle, Structural transformations in quenched Fe–Ga alloys, J. Alloys Compd. 350 (1–2) (2003) 95–101.
[80] I.S. Golovin, A.K. Mohamed, I.A. Bobrikov, A.M. Balagurov, Time-Temperature-Transformation from metastable to equilibrium structure in Fe-Ga, Mater. Lett. 263 (2020) 127257.
[81] Yue Ming Shi, Microstructural Dependence of Magnetization and Magnetostriction in Fe-20at.% Ga, Key Engineering Materials, Trans Tech Publ, 2016, pp. 100–105.
[82] Mianliang Huang, Thomas A. Lograsso, Short range ordering in Fe–Ge and Fe–Ga single crystals, Appl. Phys. Lett. 95 (17) (2009) 171907.
[83] Chaitanya Mudivarthi, Mark Laver, James Cullen, B Flatau Alison, Manfred Wuttig, Origin of magnetostriction in Fe–Ga, J. Appl. Phys. 107 (9) (2010), 09A957.
[84] A.E. Clark, M. Wun-Fogle, J.B. Restorff, Kevin W. Dennis, Thomas A. Lograsso, R William McCallum, Temperature dependence of the magnetic anisotropy and magnetostriction of Fe 100− x Ga x (x= 8.6, 16.6, 28.5), J. Appl. Phys. 97 (10) (2005) 10M316.
[85] J.R. Cullen, A.E. Clark, M. Wun-Fogle, J.B. Restorff, T.A. Lograsso, Magnetoelasticity of fe–ga and fe–al alloys, J. Magn. Magn Mater. 226 (2001) 948–949.
[86] Jayasimha Atulasimha, B Flatau Alison, James R. Cullen, Analysis of the effect of gallium content on the magnetomechanical behavior of single-crystal FeGa alloys using an energy-based model, Smart Mater. Struct. 17 (2) (2008), 025027.
[87] A.E. Clark, J.B. Restorff, M. Wun-Fogle, K.B. Hathaway, Thomas A. Lograsso, Mianliang Huang, E. Summers, Magnetostriction of ternary Fe–Ga–x (x= C, V, Cr, Mn, Co, Rh) alloys, J. Appl. Phys. 101 (9) (2007), 09C507.
[88] Liyang Dai, James Cullen, Manfred Wuttig, T. Lograsso, Eckhard Quandt, Magnetism, elasticity, and magnetostriction of FeCoGa alloys, J. Appl. Phys. 93 (10) (2003) 8627–8629.
[89] K. Aso, T. Okamoto, M. Murata, Anisotropy and magnetostriction in single crystals of new soft magnetic Fe-Ga-Si alloys, J. Phys. Colloq. 49 (C8) (1988) C8-C1905–C8-1906.
[90] Jin-liang Fan, Fang Gao, Jing-hua Liu, Effect of In, Ge addition on magnetostriction of Fe81Ga19 alloy, Heat Treat. Metals 36 (2011) 79–83.
[91] Cunzheng Dong, Menghui Li, Xianfeng Liang, Huaihao Chen, Haomiao Zhou, Xinjun Wang, Yuan Gao, Michael E. McConney, John G. Jones, Gail J. Brown, Characterization of magnetomechanical properties in FeGaB thin films, Appl. Phys. Lett. 113 (26) (2018) 262401.
[92] Xianfeng Liang, Cunzheng Dong, Sue J. Celestin, Xinjun Wang, Huaihao Chen, S Ziemer Katherine, Michael Page, Michael E. McConney, John G. Jones, Brandon M. Howe, Soft magnetism, magnetostriction, and microwave properties of Fe-Ga-C alloy films, IEEE Magn. Lett. 10 (2018) 1–5.
[93] Youwen Yang, Mingli Yang, Chongxian He, Fangwei Qi, Di Wang, Shuping Peng, Cijun Shuai, Rare earth improves strength and creep resistance of additively manufactured Zn implants, Compos. B Eng. 216 (2021).
[94] J.P. Joule, On the Effects of Magnetism upon the Dimensions of Iron and Steel Bars, Philadelphia Magazine & Journal of Science, london, 1847, p. 19.
[95] I.S. Golovin, A.M. Balagurov, V.V. Palacheva, A. Emdadi, I.A. Bobrikov, A Yu Churyumov, V.V. Cheverikin, A.V. Pozdniakov, A.V. Mikhaylovskaya, S. A. Golovin, Influence of Tb on structure and properties of Fe-19% Ga and Fe-27% Ga alloys, J. Alloys Compd. 707 (2017) 51–56.
[96] Liping Jiang, Guangrui Zhang, Jiandong Yang, Hao Hongbo, Shangxia Wu, Zengqi Zhao, Research on microstructure and magnetostriction of Fe83Ga17Dyx alloys, J. Rare Earths 28 (2010) 409–412.
[97] Xuan Zhao, Xiao Tian, Zhanquan Yao, Lijuan Zhao, Rui Wang, Jing Yan, Xinyu Liu, Flexible Pr-doped Fe–Ga composite materials: preparation, microstructure, and magnetostrictive properties, Adv. Eng. Mater. 22 (12) (2020) 2000080.
[98] Yangkun He, Xiaoqin Ke, Chengbao Jiang, Naihua Miao, Hui Wang, John Michael David Coey, Yunzhi Wang, Huibin Xu, Interaction of trace rare-earth dopants and nanoheterogeneities induces giant magnetostriction in Fe-Ga alloys, Adv. Funct. Mater. 28 (20) (2018) 1800858.
[99] Mohammad Zamanzade, Afrooz Barnoush, Christian Motz, A review on the properties of iron aluminide intermetallics, Crystals 6 (1) (2016) 10.

[100] T Pigott Miles, Iron-aluminum alloys for use in magnetostrictive transducers, J. Acoust. Soc. Am. 28 (3) (1956) 343–346.
[101] K.D. Choi, S.H. Kim, P.W. Jang, W.Y. Yoon, J.Y. Byun, Enveloping Fe–12% Al atomized powders in selectively-oxidized insulating films for soft magnetic composite (SMC) cores, J. Alloys Compd. 854 (2021) 157241.
[102] Dajun Liu, Magnetic properties of Fe-Al alloys, Shonghai Steel & Iron Res. (4) (1996) 47–53.
[103] Yongjun Han, Hui Wang, Tianli Zhang, Yangkun He, J.M.D. Coey, Chengbao Jiang, Tailoring the heterogeneous magnetostriction in Fe-Co alloys, J. Alloys Compd. 699 (2017) 200–209.
[104] Brett Sanborn, Bo Song, Susan Don, Kyle Johnson, Jeff Dabling, Jay Carroll, Brink Adam, Grutzik Scott, Andrew Kustas, Dynamic tensile behavior of soft ferromagnetic alloy Fe-Co-2V, Dynam. Behav. Mater. 1 (2020) 1–3. Springer.
[105] Shin-ichi Yamaura, Takashi Nakajima, Takenobu Satoh, Takashi Ebata, Yasubumi Furuya, Magnetostriction of heavily deformed Fe–Co binary alloys prepared by forging and cold rolling, Mater. Sci. Eng., B 193 (2015) 121–129.
[106] Xianfeng Liang, Cunzheng Dong, Huaihao Chen, Jiawei Wang, Yuyi Wei, Mohsen Zaeimbashi, Yifan He, Alexei Matyushov, Changxing Sun, Nianxiang Sun, A review of thin-film magnetoelastic materials for magnetoelectric applications, Sensors 20 (5) (2020) 1532.
[107] Jiawei Wang, Cunzheng Dong, Yuyi Wei, Xianqing Lin, Benson Athey, Yunpeng Chen, Andrew Winter, Gregory M. Stephen, Heiman Don, Yifan He, Magnetostriction, soft magnetism, and microwave properties in Co− Fe− C alloy films, Phys. Rev. Appl. 12 (3) (2019), 034011.
[108] Masaaki Sugiyama, Ryuichiro Oshima, Francisco Eiichi Fujita, Martensitic transformation in the Fe–Pd alloy system, Trans. Jpn. Inst. Metals 25 (9) (1984) 585–592.
[109] T. Kubota, T. Okazaki, Y. Furuya, T. Watanabe, Large magnetostriction in rapid-solidified ferromagnetic shape memory Fe–Pd alloy, J. Magn. Magn Mater. 239 (1–3) (2002) 551–553.
[110] A Eo Clark, Magnetostrictive rare earth-Fe2 compounds, Handb. Ferromagn. Mater. 1 (1980) 531–589.
[111] A.E. Clark, H.S. Belson, Giant room-temperature magnetostrictions in Tb Fe 2 and Dy Fe 2, Phys. Rev. B 5 (9) (1972) 3642.
[112] Deborah DL. Chung, Composite Materials for Magnetic Applications, Composite Materials, Springer, 2003, pp. 191–212.
[113] A.E. Clark, Magnetostrictive RFe2 intermetallic compounds, Handb. Phys. Chem. Rare Earths 2 (1979) 231–258.
[114] Nai-juan Wang, Yuan Liu, Hua-wei Zhang, Xiang Chen, Yan-xiang Li, Fabrication, magnetostriction properties and applications of Tb-Dy-Fe alloys: a review, China Foundry 13 (2) (2016) 75–84.
[115] Olabi Abdul-Ghani, Artur Grunwald, Design and application of magnetostrictive materials, Mater. Des. 29 (2) (2008) 469–483.
[116] J.G. Wan, J.-M. Liu, H.L.W. Chand, C.L. Choy, G.H. Wang, C.W. Nan, Giant magnetoelectric effect of a hybrid of magnetostrictive and piezoelectric composites, J. Appl. Phys. 93 (12) (2003) 9916–9919.
[117] H. Fujimori, H. Yoshimoto, T. Masumoto, T. Mitera, Anomalous eddy current loss and amorphous magnetic materials with low core loss, J. Appl. Phys. 52 (3) (1981) 1893–1898.
[118] J.A. Paulsen, A.P. Ring, C.C.H. Lo, John Evan Snyder, David C. Jiles, Manganese-substituted cobalt ferrite magnetostrictive materials for magnetic stress sensor applications, J. Appl. Phys. 97 (4) (2005), 044502.
[119] P. Martins, R. Gonçalves, S. Lanceros-Mendez, A. Lasheras, J. Gutiérrez, J. M. Barandiarán, Effect of filler dispersion and dispersion method on the piezoelectric and magnetoelectric response of CoFe2O4/P (VDF-TrFE) nanocomposites, Appl. Surf. Sci. 313 (2014) 215–219.
[120] I.H. Gul, A. Maqsood, Structural, magnetic and electrical properties of cobalt ferrites prepared by the sol–gel route, J. Alloys Compd. 465 (1–2) (2008) 227–231.
[121] M. Atif, R. Sato Turtelli, R. Grossinger, F. Kubel, Influence of manganese substitution on the microstructure and magnetostrictive properties of Co1−xMnxFe2O4 (x= 0.0–0.4) ferrite, J. Appl. Phys. 113 (15) (2013) 153902.
[122] R. Sato Turtelli, M. Kriegisch, M. Atif, R. Grössinger, Co-ferrite–A Material with Interesting Magnetic Properties, IOP Conference Series: Materials Science and Engineering, IOP Publishing, 2014, 012020.
[123] Sen-Kuan Meng, Yi-Jun Chen, Jing-Min Wang, Microstructure, Orientation and Magnetostrictive Properties of Fe 81 Ga 19 Polycrystal Grown with Bridgman Method, Rare Metals, 2019, pp. 1–5.
[124] Shekhar D. Bhame, Pattayil A. Joy, Effect of sintering conditions and microstructure on the magnetostrictive properties of cobalt ferrite, J. Am. Ceram. Soc. 91 (6) (2008) 1976–1980.
[125] Cijun Shuai, Chongxian He, Shuping Peng, Fangwei Qi, Guoyong Wang, Anjie Min, Wenjing Yang, Weiguo Wang, Mechanical alloying of immiscible metallic systems: process, microstructure, and mechanism, Adv. Eng. Mater. (2021) 2001098.
[126] J.D. Verhoeven, E.D. Gibson, O.D. McMasters, J.E. Ostenson, Directional solidification and heat treatment of Terfenol-D magnetostrictive materials, Metall. Trans. A 21 (8) (1990) 2249–2255.
[127] Xuan Zhao, Xiao Tian, Zhanquan Yao, Lijuan Zhao, Rui Wang, Hao Hongbo, Influences of growth rate on microstructures and magnetostrictive properties of Fe83Ga17 directional solidification alloys, Phil. Mag. (2020) 1–14.
[128] He Guo, Shouzeng Zhou, Zhenhua Shi, Chengbao Jiang, Qing Zhao, Preparation of rare earth-iron magnetostrictive material by directional solidification, J. Chin. Rare Earth Soc. 1 (1998).
[129] Kai Li, Wenrui Hu, Effect of non-uniform magnetic field on crystal growth by floating-zone method in microgravity, Sci. China, Ser. A: Mathematics 44 (8) (2001) 1056–1063.
[130] M.W. Vernon, M.C. Lovell, Anomalies in the electrical conductivity of nickel oxide above room temperature, J. Phys. Chem. Solid. 27 (6–7) (1966) 1125–1131.
[131] Shun Fujieda, Shigeru Suzuki, Akio Minato, Tsuguo Fukuda, Toshiyuki Ueno, Growth of Fe-Ga alloy single crystals by the Czochralski method and their application to vibration power generator, IEEE Trans. Magn. 50 (11) (2014) 1–4.
[132] S. Fujieda, R. Ukai, Y. Onuki, S. Suzuki, T. Fukuda, Influence of Co Substitution on Magnetostriction and on Young's Modulus of Fe-Ga Alloy Single Crystal, AIP Conference Proceedings, American Institute of Physics, 2015, pp. 27–31.
[133] Masahiko Ito, Kei Kamada, Akira Yoshikawa, Toru Kawamata, Shun Fujieda, Shigeru Suzuki, Tamotsu Minamitani, Toshiyuki Ueno, Shape-controlled crystal growth of Fe-Ga alloys to apply a magnetostrictive vibration energy harvester, J. Alloys Compd. 731 (2018) 898–902.
[134] J. Cui, Thomas W. Shield, Richard D. James, Phase transformation and magnetic anisotropy of an iron–palladium ferromagnetic shape-memory alloy, Acta Mater. 52 (1) (2004) 35–47.
[135] Dong-gang Wang, Xue-dao Shu, Rui Wang, Sheng Xu, Mechanism of necking defect of 6082 aluminium alloy rolled by cross-wedge rolling method based on material thermal properties, J. Cent. S. Univ. 27 (12) (2020) 3721–3732.
[136] Zhenghua He, Yuhui Sha, Fang Zhang, Feifei Lin, Liang Zuo, Development of strong η fiber recrystallization texture in rolled Fe 81 Ga 19 thin sheet, Metall. Mater. Trans. 45 (1) (2014) 129–133.
[137] X. Lu, F. Fang, Y.X. Zhang, Y. Wang, G. Yuan, Y.B. Xu, G.M. Cao, R.D.K. Misra, G. D. Wang, Evolution of microstructure and texture in grain-oriented 6.5% Si steel processed by strip-casting, Mater. Char. 126 (2017) 125–134.
[138] Quanxia Hu, Dunbo Yu, Hongchuan Yang, Kuoshe Li, Research Progress of Fe-Ga Magnetostrictive Materials, (2013).
[139] S.R. Kim, S.Y. Kang, The magnetic and magnetostrictive properties of melt-spun ribbons of B containing terfenol-D alloys, J. Magn. 2 (1) (1997) 1–6.
[140] Yangkun He, Chengbao Jiang, Wei Wu, Bin Wang, Huiping Duan, Hui Wang, Tianli Zhang, Jingmin Wang, Jinghua Liu, Zaoli Zhang, Giant heterogeneous magnetostriction in Fe–Ga alloys: effect of trace element doping, Acta Mater. 109 (2016) 177–186.
[141] Bowen Wang, Shuying Huang, Wenmei Huang, Magnetostrictive Materials and Devices, Press Metall. Industry, 2008.
[142] Sang Ho Lim, S.R. Kim, S.Y. Kang, J.K. Park, J.T. Nam, Derac son, magnetostrictive properties of polymer-bonded terfenol-D composites, J. Magn. Magn Mater. 191 (1–2) (1999) 113–121.
[143] Amorín Harvey, Miguel Algueró, Rubén Del Campo, Eladio Vila, Pablo Ramos, Mickael Dollé, Yonny Romaguera-Barcelay, Javier Pérez De La Cruz, Alicia Castro, High-sensitivity piezoelectric perovskites for magnetoelectric composites, Sci. Technol. Adv. Mater. 16 (1) (2015), 016001.
[144] Shifeng Zhao, Jian-guo Wan, Chuanfu Huang, Fengqi Song, Chang-hong Yao, Min Han, Guanghou Wang, The influence of nanoparticle size on the magnetostrictive properties of cluster-assembled Tb–Fe nanofilms, Thin Solid Films 518 (12) (2010) 3190–3193.
[145] Zhenhua Tang, Hao Ni, Biao Lu, Ming Zheng, Yong-An Huang, Sheng-Guo Lu, Minghua Tang, Ju Gao, Thickness dependence of magnetic anisotropy and domains in amorphous Co40Fe40B20 thin films grown on PET flexible substrates, J. Magn. Magn Mater. 426 (2017) 444–449.
[146] Uta Allenstein, Emilia I. Wisotzki, Christine Graefe, Joachim H. Clement, Yanhui Liu, Schroers Jan, Stefan G. Mayr, Binary Fe-Pd submicron structures fabricated through glancing angle deposition (GLAD) for bioapplications, Mater. Des. 131 (2017) 366–374.
[147] Takashi Matsumae, Masahisa Fujino, Tadatomo Suga, Room-temperature bonding method for polymer substrate of flexible electronics by surface activation using nano-adhesion layers, Jpn. J. Appl. Phys. 54 (10) (2015) 101602.
[148] M Hughes, What Is Sputtering? Magnetron Sputtering, Semicore. Published November 24 (2014).
[149] N.B. Ekreem, A.G. Olabi, T. Prescott, A. Rafferty, M.S.J. Hashmi, An overview of magnetostriction, its use and methods to measure these properties, J. Mater. Process. Technol. 191 (1–3) (2007) 96–101.
[150] Qi-han Xia, Testing principle of the strain gauge and its application in the practical engineering [J], Shanxi Architect. 28 (2008).
[151] Wei Wang, Huiming Liu, Rongjin Huang, Yuqiang Zhao, Chuangjun Huang, Shibin Guo, Yi Shan, Laifeng Li, Thermal expansion and magnetostriction measurements at cryogenic temperature using the strain gauge method, Front. Chem. 6 (2018) 72.
[152] R. Küchler, T. Bauer, M. Brando, F. Steglich, A compact and miniaturized high resolution capacitance dilatometer for measuring thermal expansion and magnetostriction, Rev. Sci. Instrum. 83 (9) (2012), 095102.
[153] G.K. White, Thermal expansion at low temperatures. II. Electronic component in metals, Phil. Mag. 6 (66) (1961) 815–818.
[154] Devishvili Anton, Martin Rotter, Andreas Lindbaum, Barcza Alexander, Arno Hiess, Wolfgang Schmidt, Vejpravova Jana, Measuring magnetostriction with neutrons, J. Phys. Condens. Matter 20 (10) (2008) 104218.
[155] H. Samata, Y. Nagata, T. Uchida, S. Abe, New optical technique for bulk magnetostriction measurement, J. Magn. Magn Mater. 212 (3) (2000) 355–360.
[156] K. Kakuno, Y. Gondó, A new measuring method of magnetostrictive vibration, J. Appl. Phys. 50 (B11) (1979) 7713–7715.
[157] J.C.M. Henning, J.H. Den Boef, Magnetostriction measurement by means of strain modulated ferromagnetic resonance (SMFMR), Appl. Phys. 16 (4) (1978) 353–357.

[158] A. Mitra, M. Vázquez, Measurement of the saturation magnetostriction constant of amorphous wire, J. Appl. Phys. 67 (9) (1990) 4986–4988.
[159] M. Churyukanova, V. Semenkova, S. Kaloshkin, E. Shuvaeva, S. Gudoshnikov, V. Zhukova, I. Shchetinin, A. Zhukov, Magnetostriction investigation of soft magnetic microwires, Phys. Status Solidi 213 (2) (2016) 363–367.
[160] Michał Nowicki, Stress dependence of the small angle magnetization rotation signal in commercial amorphous ribbons, Materials 12 (18) (2019) 2908.
[161] Hal R. Holmes, Eli Vlaisavljevich, Ee Lim Tan, Katherine L. Snyder, Keat Ghee Ong, Rupak M. Rajachar, Control of cellular adhesion and myofibroblastic character with sub-micrometer magnetoelastic vibrations, J. Biomech. 71 (2018) 199–207.
[162] Y. Ma, M. Zink, S.G. Mayr, Biocompatibility of single crystalline Fe 70 Pd 30 ferromagnetic shape memory films, Appl. Phys. Lett. 96 (21) (2010) 213703.
[163] Pierre Pouponneau, Yahye Merhi, Laura Mery Epure, Sylvain Martel, Biocompatibility of candidate materials for the realization of medical microdevices, in: International Conference of the IEEE Engineering in Medicine and Biology Society, IEEE, 2006, pp. 2362–2365.
[164] Guoyong Wang, Guowen Qian, Jun Zan, Fangwei Qi, Zhengyu Zhao, Wengjing Yang, Shuping Peng, Cijun Shuai, A co-dispersion nanosystem of graphene oxide@ silicon-doped hydroxyapatite to improve scaffold properties, Mater. Des. 199 (2021) 109399.
[165] Henan Wang, Yang Zheng, Jinghua Liu, Chengbao Jiang, Yan Li, In vitro corrosion properties and cytocompatibility of Fe-Ga alloys as potential biodegradable metallic materials, Mater. Sci. Eng. C 71 (2017) 60–66.
[166] Vera N. Malheiro, Rose L. Spear, Roger A. Brooks, Athina E. Markaki, Osteoblast and monocyte responses to 444 ferritic stainless steel intended for a magneto-mechanically actuated fibrous scaffold, Biomaterials 32 (29) (2011) 6883–6892.
[167] Cijun Shuai, Xun Yuan, Wenjing Yang, Shuping Peng, Guowen Qian, Zhenyu Zhao, Synthesis of a mace-like cellulose nanocrystal@ Ag nanosystem via in-situ growth for antibacterial activities of poly-L-Lactide scaffold, Carbohydr. Polym. (2021) 117937.
[168] Cijun Shuai, Jun Zan, Fang Deng, Youwen Yang, Shuping Peng, Zhenyu Zhao, Core–shell-structured ZIF-8@ PDA-HA with controllable Zinc ion release and superior bioactivity for improving a poly-l-lactic acid scaffold, ACS Sustain. Chem. Eng. 9 (4) (2021) 1814–1825.
[169] V.N. Malheiro, J.N. Skepper, R.A. Brooks, A.E. Markaki, In vitro osteoblast response to ferritic stainless steel fiber networks for magneto-active layers on implants, J. Biomed. Mater. Res. 101 (6) (2013) 1588–1598.
[170] H Vining Kyle, David J. Mooney, Mechanical forces direct stem cell behaviour in development and regeneration, Nat. Rev. Mol. Cell Biol. 18 (12) (2017) 728–742.
[171] Wendy M. Kohrt, Susan A. Bloomfield, Kathleen D. Little, Miriam E. Nelson, R Yingling Vanessa, Physical activity and bone health, Med. Sci. Sports Exerc. 36 (11) (2004) 1985–1996.
[172] Yi-Xian Qin, Clinton T. Rubin, Kenneth J. McLeod, Nonlinear dependence of loading intensity and cycle number in the maintenance of bone mass and morphology, J. Orthop. Res. 16 (4) (1998) 482–489.
[173] Charles H. Turner, M.R. Forwood, J.-Y. Rho, T. Yoshikawa, Mechanical loading thresholds for lamellar and woven bone formation, J. Bone Miner. Res. 9 (1) (1994) 87–97.
[174] Fangwei Qi, Zichao Zeng, Yao Jia, Weiliang Cai, Zhenyu Zhao, Shuping Peng, Cijun Shuai, Constructing Core-Shell Structured BaTiO3 @carbon Boosts Piezoelectric Activity and Cell Response of Polymer Scaffolds, Mater. Sci. Eng. C (2021).
[175] Shuji Taue, Yasuyuki Sugihara, Tetsuo Kobayashi, Sunao Ichihara, Kiyoshi Ishikawa, Natsuhiko Mizutani, Development of a highly sensitive optically pumped atomic magnetometer for biomagnetic field measurements: a phantom study, IEEE Trans. Magn. 46 (9) (2010) 3635–3638.
[176] Dmitry Murzin, Desmond J. Mapps, Kateryna Levada, Victor Belyaev, Omelyanchik Alexander, Larissa Panina, Valeria Rodionova, Ultrasensitive magnetic field sensors for biomedical applications, Sensors 20 (6) (2020) 1569.
[177] Dwight Viehland, Manfred Wuttig, Jeffrey McCord, Eckhard Quandt, Magnetoelectric magnetic field sensors, MRS Bull. 43 (11) (2018) 834–840.
[178] Jens Reermann, Phillip Durdaut, Sebastian Salzer, Thomas Demming, André Piorra, Eckhard Quandt, Norbert Frey, Michael Höft, Gerhard Schmidt, Evaluation of magnetoelectric sensor systems for cardiological applications, Measurement 116 (2018) 230–238.
[179] Limin Ren, Kun Yu, Yisong Tan, Monitoring and assessing the degradation rate of magnesium-based artificial bone in vitro using a wireless magnetoelastic sensor, Sensors 18 (9) (2018) 3066.
[180] Mohsen Zaeimbashi, Hwaider Lin, Cunzheng Dong, Xianfeng Liang, Mehdi Nasrollahpour, Huaihao Chen, Neville Sun, Alexei Matyushov, Yifan He, Xinjun Wang, NanoNeuroRFID, A wireless implantable device based on magnetoelectric antennas, IEEE J. Electromagn. RF Microw. Med. Biol. 3 (3) (2019) 206–215.
[181] Huaihao Chen, Xianfeng Liang, Neville Sun, Nian-Xiang Sun, Hwaider Lin, Yuan Gao, An ultra-compact ME antenna design for implantable wireless communication, in: IEEE International Symposium on Antennas and Propagation and North American Radio Science Meeting, IEEE, 2020, pp. 655–656.
[182] F. Rangriz, A. Khaleghi, I. Balasingham, Wireless link for micro-scale biomedical implants using magnetoelectric antennas, in: 14th European Conference on Antennas and Propagation (EuCAP), IEEE, 2020, pp. 1–4.